

Institutionen för systemteknik

Department of Electrical Engineering

Examensarbete

Optimization of Fuel Consumption in a Hybrid Powertrain

Examensarbete utfört i Fordonssystem
vid Tekniska högskolan vid Linköpings universitet
av

Martin Sivertsson

LiTH-ISY-EX--10/4376--SE

Linköping 2010



Linköpings universitet
TEKNISKA HÖGSKOLAN

Optimization of Fuel Consumption in a Hybrid Powertrain

Examensarbete utfört i Fordonssystem
vid Tekniska högskolan i Linköping
av

Martin Sivertsson

LiTH-ISY-EX--10/4376--SE

Handledare: **Ph.D. Student Christofer Sundström**
ISY, Linköpings universitet

Pierre Petterson
Haldex Traction AB

Examinator: **Associate Professor Lars Eriksson**
ISY, Linköpings universitet

Linköping, 14 December, 2010

	Avdelning, Institution Division, Department Division of Automatic Control Department of Electrical Engineering Linköpings universitet SE-581 83 Linköping, Sweden	Datum Date 2010-12-14
Språk Language <input type="checkbox"/> Svenska/Swedish <input checked="" type="checkbox"/> Engelska/English <input type="checkbox"/> _____	Rapporttyp Report category <input type="checkbox"/> Licentiatavhandling <input checked="" type="checkbox"/> Examensarbete <input type="checkbox"/> C-uppsats <input type="checkbox"/> D-uppsats <input type="checkbox"/> Övrig rapport <input type="checkbox"/> _____	ISBN _____ ISRN LiTH-ISY-EX--10/4376--SE Serietitel och serienummer ISSN Title of series, numbering _____
URL för elektronisk version http://www.fs.isy.liu.se http://www.ep.liu.se		
Titel Optimering av bränsleförbrukning i en hybrid drivlina Title Optimization of Fuel Consumption in a Hybrid Powertrain Författare Martin Sivertsson Author		
Sammanfattning Abstract <p>Increased environmental awareness together with new legislative demands on lowered emissions and a rising fuel cost have put focus on increasing the fuel efficiency in new vehicles. Hybridization is a way to increase the efficiency of the powertrain. The Haldex electric Torque Vectoring Device is a rear axle with a built in electric motor, designed to combine all-wheel drive with hybrid functionality. A method is developed for creating a real time control algorithm that minimizes the fuel consumption. First the consumption reduction potential of the system is investigated using Dynamic Programming. A real time control algorithm is then devised that indicates a substantial consumption reduction potential compared to all-wheel drive, under the condition that the assumed and measured efficiencies are accurate. The control algorithm is created using equivalent consumption minimization strategy and is implemented without any knowledge of the future driving mission. Two ways of adapting the control according to the battery state of charge are proposed and investigated. The controller optimizes the torque distribution for the current gear as well as assists the driver by recommending the gear which would give the lowest consumption. The simulations indicate a substantial fuel consumption reduction potential even though the system primarily is an all-wheel drive concept. The results from vehicle tests show that the control system is charge sustaining and the driveability is deemed good by the test-drivers.</p>		
Nyckelord Keywords Hybrid Electric Vehicles, Dynamic Programming, Equivalent Consumption Minimization Strategy		

Abstract

Increased environmental awareness together with new legislative demands on lowered emissions and a rising fuel cost have put focus on increasing the fuel efficiency in new vehicles.

Hybridization is a way to increase the efficiency of the powertrain. The Haldex electric Torque Vectoring Device is a rear axle with a built in electric motor, designed to combine all-wheel drive with hybrid functionality. A method is developed for creating a real time control algorithm that minimizes the fuel consumption. First the consumption reduction potential of the system is investigated using Dynamic Programming. A real time control algorithm is then devised that indicates a substantial consumption reduction potential compared to all-wheel drive, under the condition that the assumed and measured efficiencies are accurate. The control algorithm is created using equivalent consumption minimization strategy and is implemented without any knowledge of the future driving mission. Two ways of adapting the control according to the battery state of charge are proposed and investigated. The controller optimizes the torque distribution for the current gear as well as assists the driver by recommending the gear which would give the lowest consumption. The simulations indicate a substantial fuel consumption reduction potential even though the system primarily is an all-wheel drive concept. The results from vehicle tests show that the control system is charge sustaining and the driveability is deemed good by the test-drivers.

Acknowledgements

From ISY, department of Vehicular Systems at Linköping University, I would like to thank my supervisor, Ph.D. Student Christofer Sundström and examiner Associate Professor Lars Eriksson for their advice and help throughout this thesis.

At Haldex I would like to thank my supervisor Pierre Pettersson for his help and participation, making this thesis possible, and also department director Daniel Hervén for giving me the opportunity to contribute to such an interesting system.

“Hybrids began where EVs ended.”

– Dr Takehisa Yaegashi, Senior General Manager, Powertrain Development Group, Toyota Motor Corporation

Table of Contents

1	Introduction	1
1.1	Problem Formulation	1
1.2	Outline.....	1
1.3	Driving Cycles	2
2	Hybrid Vehicles	3
2.1	Hybrid Electric Vehicles.....	4
2.1.1	Series Hybrid	4
2.1.2	Parallel Hybrid	5
2.1.3	Split Hybrid:.....	5
2.2	The Haldex eTVD Hybrid and the test vehicle.....	6
3	Control Strategies	7
3.1	Deterministic Dynamic Programming	7
3.2	Analytical Dynamic Optimization.....	9
3.3	Adaptive Control	10
3.3.1	Update according to the SOC.....	10
4	Vehicle and Component Modeling	11
4.1	Longitudinal Vehicle Model	11
4.2	Component Modeling	13
4.2.1	Energy Converters.....	13
4.2.2	Transmission	13
4.2.3	Clutch	14
4.2.4	Battery.....	15
4.2.5	Powertrain	18
5	Reference Consumption	19
6	Dynamic Programming.....	21
6.1	Calculations	21
6.2	Results.....	21
6.2.1	NEDC	21
6.2.2	FTP-75	23
6.2.3	Stability analysis.....	25
7	Equivalent Consumption Minimization Strategy	27
7.1	Pre-Calculations	27
7.2	Implementation	30

7.2.1	The Gear Selector.....	30
7.2.2	The ECMS block.....	31
7.3	Simulation Results.....	32
7.3.1	Analysis and Interpretation of NEDC Results.....	32
7.3.2	Analysis and Interpretation of FTP-75 Results.....	34
7.3.3	ECMS evaluation.....	36
7.4	Prediction of the Equivalence Factor.....	36
7.4.1	Static Prediction based on SOC.....	37
7.4.2	Results with Static Prediction based on SOC.....	39
7.4.3	Adaptive Prediction based on SOC.....	40
7.5	System performance on unknown cycles.....	43
7.5.1	The ECMS with Static Prediction based on SOC.....	43
7.5.2	The ECMS with Adaptive Prediction based on SOC.....	44
7.5.3	Evaluation.....	44
8	Vehicle Tests.....	45
9	Conclusion.....	49
9.1	Future Work.....	49
10	References.....	51

1 Introduction

Increased environmental awareness together with new legislative demands on lowered emissions and a rising fuel cost has put more focus on increasing the overall fuel efficiency in new vehicles. The key elements in increasing the overall fuel efficiency are:

- To optimize the powertrain components. Reducing the losses in components such as combustion engine and transmission is a first step to lowering consumption, and thus emissions.
- To optimize the powertrain configuration. By adding extra components, i.e. hybridize the vehicle, the overall efficiency of the powertrain can be increased.
- To optimize the control algorithm. Especially for more advanced systems, such as hybrids, it's important to make sure that the control system uses the components in an efficient way.

A gasoline internal combustion engine (ICE) on average only operates at around 17% efficiency in a conventional vehicle [3], to be compared with a peak efficiency of around 37%. This is due to the fact that under normal driving conditions the ICE is operated at part load, where the efficiency is low. A hybrid vehicle offers a way to utilize the ICE in a more efficient way and thus increase the overall efficiency of the vehicle.

1.1 Problem Formulation

Haldex Traction AB is currently developing a rear axle with an integrated electric motor, the Haldex electric Torque Vectoring Device (eTVD). The aim is to be able to combine all-wheel drive (AWD), with hybrid functionality. The purpose of this Master's Thesis is to develop a supervisory control algorithm for the Haldex eTVD Powertrain system that minimizes the fuel consumption, while being charge sustaining. Since the developed control algorithm is to be implemented in a future real-time control system it has to fulfill requirements on robustness, accuracy and computational effort. Due to Haldex position as a subcontractor to the vehicle industry, the devised algorithm also has to be highly adaptable to a variety of vehicles, with a minimum of tuning work.

1.2 Outline

Sections 2 and 3 are the literature study, where Section 2 covers the main hybrid architectures and Section 3 the some of the available control algorithms.

The vehicle is then modeled in Section 4 before two different reference consumptions are calculated, first the consumption as an AWD vehicle in Section 5 and then an approximation of the minimum consumption achievable in the hybrid configuration in Section 6. In Section 7 the real time control algorithm is created using Equivalent Consumption Minimization Strategy (ECMS) and evaluated. The controller is then tested in a vehicle in Section 8.

1.3 Driving Cycles

A driving cycle is a standardized velocity profile used to compare the performance regarding fuel consumption and pollutant emissions between different vehicles. Several countries and organizations have developed their own driving cycles to reflect the ways a vehicle is being used in that region.

In Europe the standard driving cycle for certification is the New European Driving Cycle (NEDC). It consists of four repetitions of an urban driving pattern and one extra-urban driving pattern. The driving cycle is supposed to model how a car is normally being used in Europe [11].

In the USA the standard driving cycle is the Federal Test Procedure 75 (FTP-75). The cycle consists of three phases: The cold start phase (0-505s), the transient phase (505-1369s) and the hot start phase (1369s-) [12].

Both the FTP-75 and the NEDC cycles are shown in Fig 1. The velocity profiles are quite different from each other. They are later used to evaluate the proposed control algorithms, both regarding charge sustenance and fuel consumption.

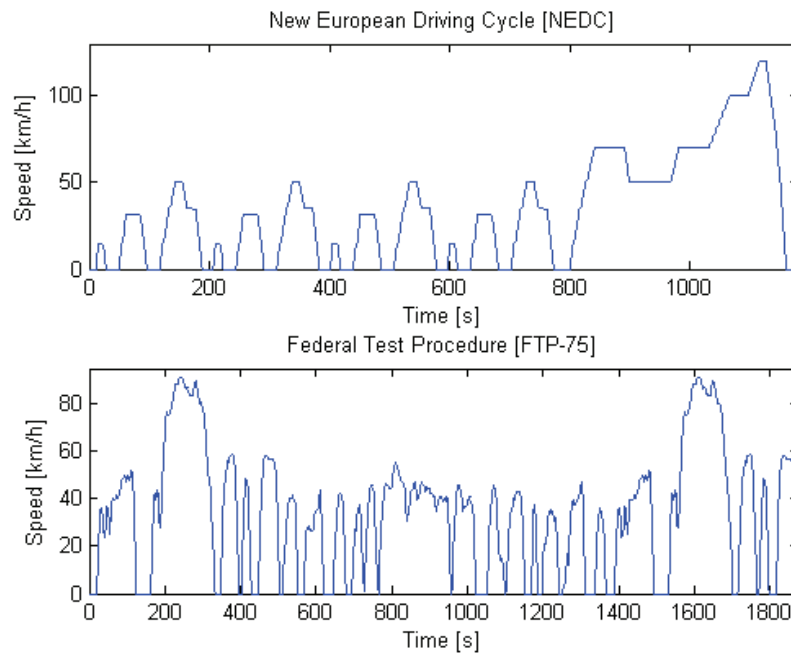


Fig 1 The NEDC and FTP-75 driving cycles. The two velocity profiles are used to evaluate the control algorithms.

2 Hybrid Vehicles

A hybrid powertrain utilizes at least two separate energy converters. Normally the ICE [1] is the primary converter and a non-combustion energy converter is used as a secondary converter. This provides some advantages compared to the conventional powertrain:

- **Load Shift/Optimize Energy Distribution:** The Hybrid configuration provides a freedom in choosing the operating points of the components in the vehicle. In a conventional powertrain the torque demanded from the driver (T_{dem}) has to be met by the ICE, $T_{dem}=T_{ICE}$. With two energy converters the ICE is assisted by a secondary energy converter, $T_{dem}=T_{ICE}+T_{secondary}$. Since the secondary converter can charge the energy storage through a negative torque as well as assist the ICE with a positive torque, the operating point of the ICE can be shifted to a region with higher efficiency. This is most common at low loads since the efficiency of the ICE is particularly poor in the low load region, see Fig 2, but can also be done at high loads. The extra degree of freedom through hybridization provides the possibility to choose when to use which converter and thus use the system as efficiently as possible.

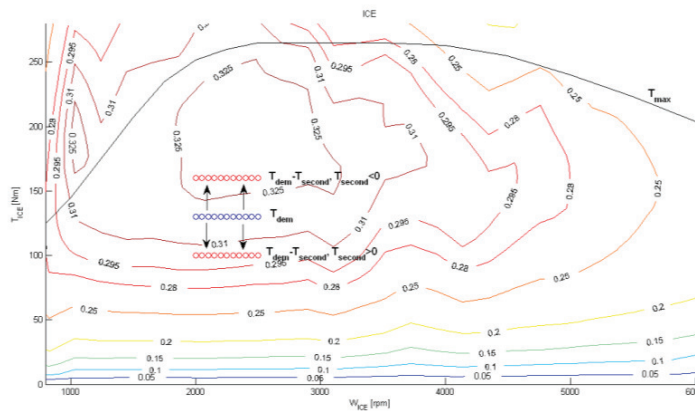


Fig 2 Load shift. Through a torque from the secondary converter or generator it is possible to use the ICE in a more efficient way. The lines represent the different efficiency regions of the ICE.

- **Regenerative braking:** The ability to recuperate some of the kinetic energy during braking for later use by the secondary converter.
- **Stop and go:** Turning off the ICE while idling eliminates the idle fuel consumption.
- **Downsizing:** With two or more energy converters the ICE doesn't have to be dimensioned for the most demanding acceleration scenario. Instead this scenario is covered by the sum of the power available from all converters. Therefore it is possible to use a smaller ICE without affecting the performance of the vehicle. Since the efficiency of a smaller ICE at a given operating point in general is higher than that of a larger ICE, this increases the overall efficiency. However, downsizing reduces the long term hill climbing ability and the top speed of the vehicle.

The main disadvantages of hybridization are increased weight and cost of the vehicle.

2.1 Hybrid Electric Vehicles

Hybrid vehicles are divided into three main hybrid architectures [10]: Series hybrid, Parallel hybrid and Split hybrid. These architectures aren't specific for Hybrid Electric Vehicles (HEV); instead they are a description of the energy paths available. But since HEV, where the ICE is used in combination with an electric motor (EM), is the most common hybrid type [1] and also the category the eTVD falls under, the following description of the characteristics of the three different architectures is done on HEVs.

2.1.1 Series Hybrid

A series hybrid consists of two EMs and an ICE. One EM acts purely as a generator and the other as a generator, during regenerative braking, as well as traction motor. The ICE acts purely as an auxiliary power unit that charges the battery; hence the vehicle is primarily an electric vehicle. The architecture of the series hybrid is shown in Fig 3. The benefit of having the ICE speed decoupled from the wheel speed is the possibility to always run the ICE at its most efficient operating point in regard to fuel consumption and emission. Because of this the system is efficient in stop and go driving situations, i.e. urban traffic, since the ICE isn't affected by the varying speed and power demand from the driver. However, in high speed driving, the bulk of the energy used by the traction motor comes from the ICE instead of from regenerative braking and there's not as much to be gained from optimizing the operating points of the ICE. Instead the extra conversion step introduced between the ICE and the wheels result in fairly low overall efficiency.

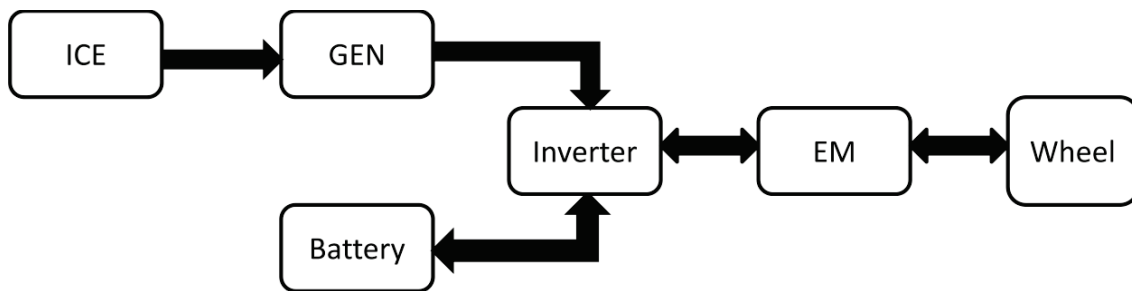


Fig 3 Schematic overview of the series hybrid. In a series hybrid the ICE acts purely as an auxiliary power unit to provide energy to the electrical traction motor.

2.1.2 Parallel Hybrid

In a parallel hybrid both the ICE and the EM has a mechanical connection to both the wheels and to each other. Since the wheel speed and ICE speed are coupled through the gear box the operating points of the ICE can only be chosen for a discrete set of ICE speeds. It also makes charging the battery while standing still impossible. The architecture is shown in Fig 4. Even though a parallel hybrid isn't as efficient in urban driving as the series hybrid, it has the advantage of not always having to convert the produced power to electricity. In high demanding driving situations, i.e. highway, it can be driven purely as a conventional vehicle. Since the ICE has a connection to the wheels the EM does not have to be as large as in the series hybrid case.

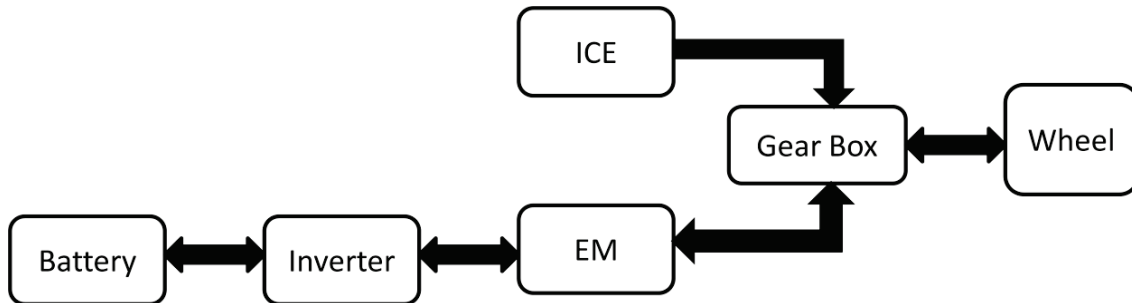


Fig 4 Schematic overview of the parallel hybrid. In a parallel hybrid the ICE has a mechanical connection both to the EM and to the wheels.

2.1.3 Split Hybrid:

In a split hybrid the configuration is as in the series hybrid with the addition that the ICE is also connected to the wheels. This configuration can, if correctly dimensioned, avoid the drawbacks of the series and parallel concepts [1]. The architecture is shown in Fig 5. Since the split hybrid can be operated both as a series hybrid and a parallel hybrid, it is sometimes known as a series-parallel hybrid. The added complexity of the system and the number of components increases the cost, weight and developmental effort needed.

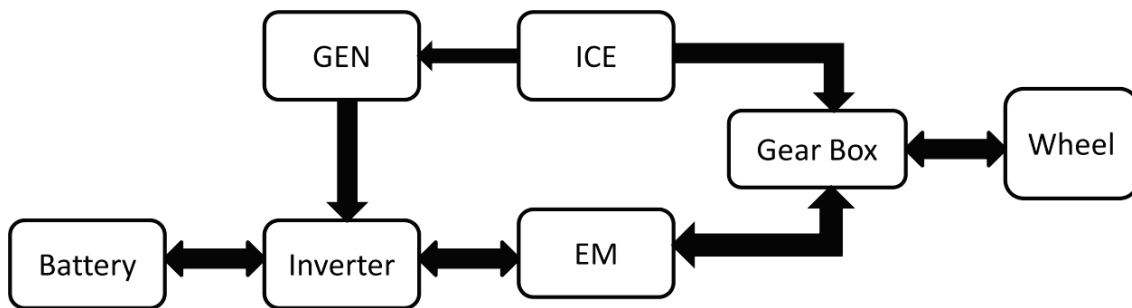


Fig 5 Schematic overview of the split hybrid. In a split hybrid there are two energy paths from the ICE to the wheels and EM, one mechanical through the gear box, and one electrical through the generator. This has the potential of avoiding the drawbacks of the parallel and series hybrids.

2.2 The Haldex eTVD Hybrid and the test vehicle

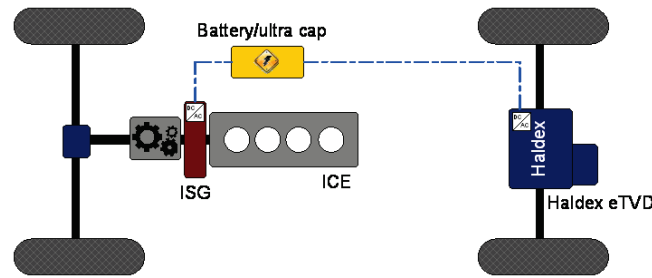


Fig 6 Schematic overview of the Haldex eTVD system. The ICE has a mechanical connection to the EM via the wheels and an electrical connection via the ISG.

The Haldex eTVD is a system designed to combine all-wheel drive (AWD) with hybrid functionality. The main difference between the Haldex eTVD and a normal hybrid is the all-wheel drive functionality. It also has the ability to control the torque distribution on the rear wheels individually, which is useful to prevent under- and over-steering.

In the Haldex eTVD the ICE and EM are connected electrically to each other via the Integrated Starter and Generator (ISG) and mechanically via the wheels. The architecture, shown in Fig 6, of the system thus resembles that of a split hybrid but since the components in the prototype are dimensioned for AWD the series hybrid functionality of the vehicle is reduced. A more fitting description would be advanced parallel hybrid since it can be viewed as a parallel hybrid with an extra degree of freedom in choosing which energy converter to use during load shifting since the ISG is added to the powertrain.

Since the concept is still in the prototype stage the control of the test vehicle has some limitations. The only controllable signal is the torque distribution between the ICE, ISG and EM, but only when a gear is engaged. This means that engine shut off during idle as well as driving while the ICE is turned off or idling is not possible.

The test vehicle is a SAAB 9-3 XWD with a 2.0 litre turbo charged spark ignited combustion engine and a six-speed manual gear box (GB).

3 Control Strategies

The objective in HEV control is to minimize the fuel consumption over a driving cycle. One solution to this is all-electric drive, providing that the driving cycle is short enough. In a global perspective, fully depleting the battery not only damages the battery but also forces the system to either recharge the battery under potentially suboptimal conditions or the hybrid functionality will be lost. Therefore the real objective is not only to minimize fuel consumption, but also to maintain the battery State of Charge (SOC) within certain limitations; the control algorithm has to be charge sustaining.

The problem is to find the solution that minimizes the fuel consumption over a driving cycle while maintaining the SOC within the prescribed limits. This can be written as [4]:

$$J = \min \left(\int_0^T \dot{m}_f(t, u(t)) dt + \phi(SOC(T)) \right) \quad (1)$$

Where $\dot{m}_f(t, u(t))$ is the fuel flow to the ICE, u is a variable that describes the power split between the different energy converters and ϕ is a function that penalizes deviations in the final SOC.

There are two main branches of hybrid control system design. The rule-based control, that relies on heuristic knowledge of the system, as described in [3, 6], and various optimization methods. Beside the two optimization methods described in this report the most notable are the Static Optimization described in [4] and the Stochastic Dynamic Programming described in [10].

3.1 Deterministic Dynamic Programming

Deterministic Dynamic Programming (DDP), as described in [1-4, 6], is a model based multi-stage decision process that can be used to find the optimal trajectory of a control variable over a pre-defined driving cycle. It requires the control states and time to be discretized and thus the global optimum is only guaranteed to grid accuracy.

Fig 7 shows the first steps of the algorithm. The SOC is discretized and a cost is assigned to all final values of SOC. This cost acts as an end constraint on SOC and can be done both as a hard and a soft constraint. A hard constraint is represented with an infinite cost.

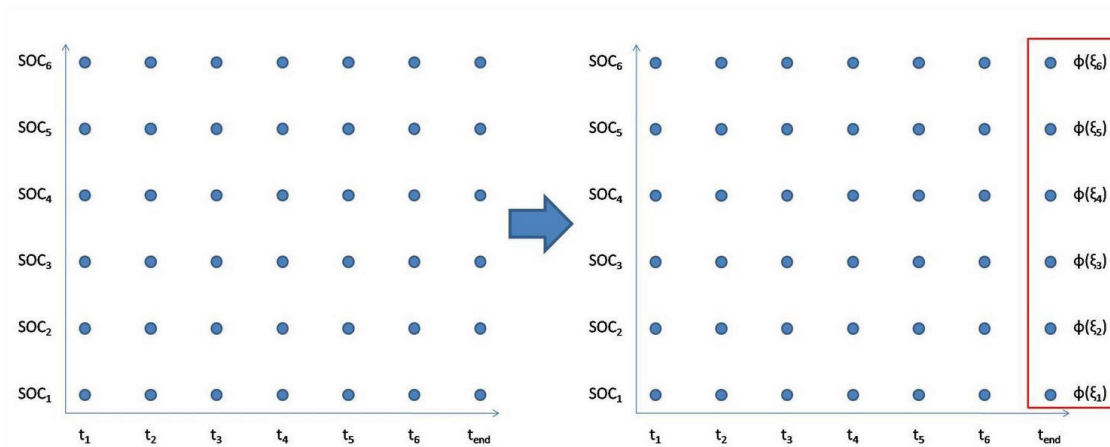


Fig 7 The SOC and time is discretized and a cost is assigned to all possible end values in SOC

The cost, in fuel consumption, to go from t_{n-1} to t_n is calculated for all possible starting values in SOC and end SOC.

In Fig 8 the algorithm iterates through one time step for all values in SOC. Each iteration calculates the cost in fuel, $f(\Delta t, SOC)$, to go from the start SOC to all possible end values in SOC.

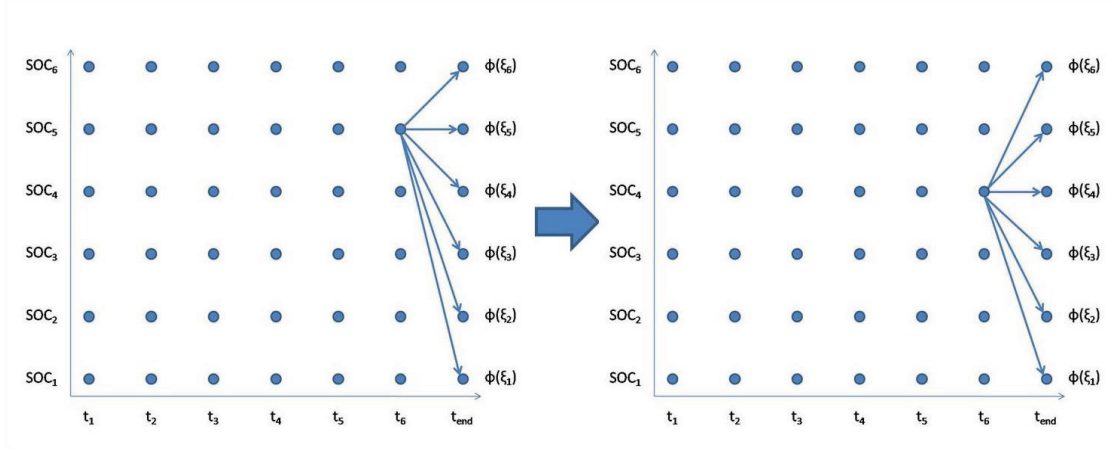


Fig 8 The cost to go from one start SOC to all end SOC is evaluated. This is repeated for all start SOC.

The arcs are evaluated subject to all local and global constraints. Thus all values in SOC aren't reachable from all starting SOC, e.g. due to large currents or torque limits.

The cost associated with reaching the end SOC, $\Gamma(t + \Delta t, SOC)$, is then added to the cost for the arc leading up to that SOC, as shown in Fig 9. Thus, in each iteration the cost of going from the current time to the end of the cycle is calculated and the arc with the lowest cost is saved.

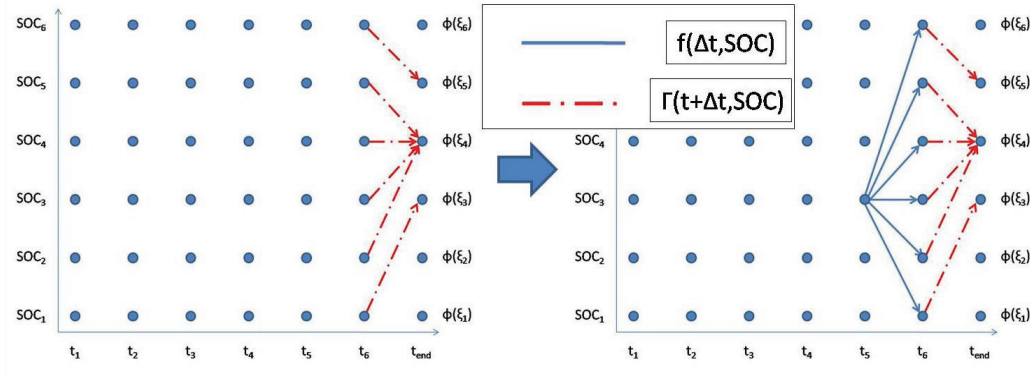


Fig 9 For each start SOC, in the current time step, the best end SOC is stored. The cost for that step is then added to all the steps that lead to that particular start SOC.

The algorithm iterates through all time steps, from last to first, saving the arcs with the minimum cost according to:

$$\Gamma(t, SOC) = f(\Delta t, SOC_{opt}) + \Gamma(t + \Delta t, SOC_{opt}) \quad (2)$$

Where $f(\Delta t, SOC)$, solid lines, is the cost for that particular SOC and time step and $\Gamma(t + \Delta t, SOC)$, dash-dotted lines, is the cost associated with going from the end SOC in that time step to the end of the driving cycle.

The computational burden of the algorithm increases linearly with the cycle-time and exponentially with the size of the discretization of the control variables [4]. Because of the computational intensity due to the size of the discretization, a rule extracting-phase normally has to be used in order to transform this into a real-time controller. The control system is still only valid for the driving cycle for which it was designed for since the entire driving cycle has to be known [1].

3.2 Analytical Dynamic Optimization

As discussed in the previous chapter numerical optimization is a reliable way of finding the optimal control strategy. But the computational intensity and the need for knowledge of the future driving mission limits the possibility of using this approach in a real time controller. Another approach is to try to transform the optimization problem to something more manageable, to try and make use of the knowledge of the system instead of relying on brute force. One such approach is the ECMS [1-4, 6-8].

The main idea in ECMS is that instead of searching for a global optimum for a driving mission, the torque distribution that minimizes the sum of power from fuel and power from the battery is selected. Since power from fuel and battery power aren't directly comparable an equivalence factor is needed, which corresponds to the adjoint state in classical optimization theory [3]. The assumption is that all used battery energy has to be recharged by the ICE at the current operating point. The adjoint state thus represents the average of the energy paths from the fuel to the battery [7]. The benefit of this problem formulation is that it drastically reduces the computational time and simplifies adaptive control, since the controlling parameter is the adjoint state.

The Hamiltonian function to be minimized that represents the minimization problem is on the form [4]:

$$H(t, s(t), u, v) = P_f(t, u, v) + \lambda(t)P_{batt}(t, u, v) \quad (3)$$

Where:

- $\lambda(t)$ is the equivalence factor
- u is the power split control variable
- v is the vehicle speed
- P_f is the power from fuel
- P_{batt} is the power from the battery is the maximum battery capacity

It can be seen that this instantaneous optimization problem is not the same as global optimization, but it can easily be used for real-time control [1]. Under the assumption that the battery efficiency is constant for all SOC, the adjoint state λ remains approximately constant along the optimal trajectory [4, 6]. Therefore the optimization problem is reduced to finding the constant λ that approximates the optimal trajectory of a given driving cycle. Since the characteristics of the battery are different depending on if the battery is charging or discharging λ is often replaced by two constants [1-3, 6-7]. It is however shown that one constant suffices to get a good approximation on a given driving cycle [7].

3.3 Adaptive Control

Even though several of the suggested optimization strategies produce good results on a given drive-cycle they do not guarantee charge sustenance in a real-time implementation. For this to be achieved the control states have to be updated according to the driving missions.

To ensure that the solution is close to optimum, the driving conditions ahead must be known. There exists several solutions to this. For example the A-ECMS suggested in [4,7] where the velocity profile is calculated from a GPS signal or the T-ECMS [4] where radar information is used together with a GPS signal to predict the future mission. Another option, under the assumption that the past driving conditions are valid for the near future, is the pattern recognition suggested in [9].

Since the test vehicle has no equipment to predict the future conditions mainly two options are of interest, pattern recognition and update according to SOC described below.

3.3.1 Update according to the SOC

The idea is to penalize deviations in SOC, as suggested in [10]. This will have the effect that extensive use of battery power will cause the system to favor the ICE over the EM and vice versa. In (1) this constraint is enforced only on the end SOC, but to make sure that the control system stays within the specified boundaries it is applied on all time steps. Although this does not ensure optimality, it at least increases charge sustenance.

4 Vehicle and Component Modeling

For the purpose of investigating different control strategies and their fuel consumptions a quasistatic model approach is selected. In a backward facing quasistatic approach the speed is known from the driving cycle. When the speed is known the torque required at the wheels to follow the driving cycle is calculated through a longitudinal vehicle model. The schematics of the system are shown in Fig 10. In order to calculate the control signals, i.e. the torques T_{ICE} , T_{ISG} , T_{EM} and the gear γ_{GB} , the vehicle and its components have to be modeled.

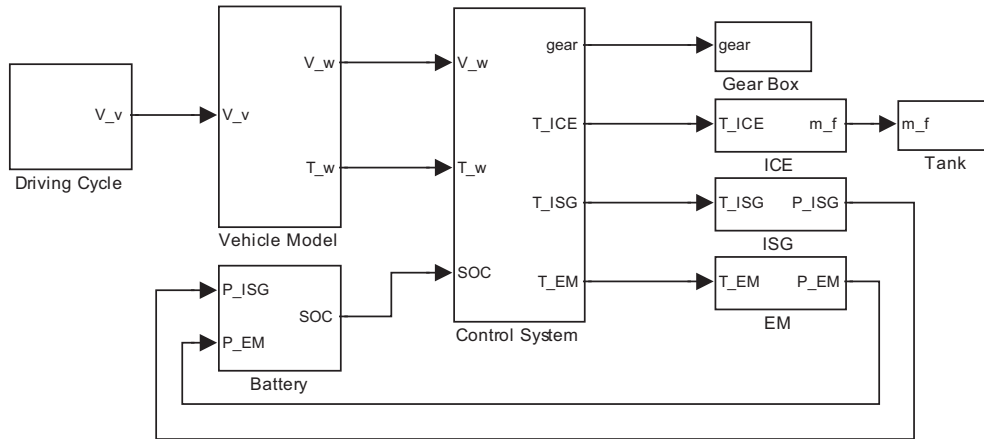


Fig 10 The schematics of the system. For a given speed and SOC the gear and torques on the individual converters are decided.

The modeling equations described in the following sections are from [3].

4.1 Longitudinal Vehicle Model

Since only the power split between the ICE, ISG and EM is of interest, a longitudinal vehicle model, as seen in Fig 11, is used to simulate the required torque at the wheels for a given driving cycle.

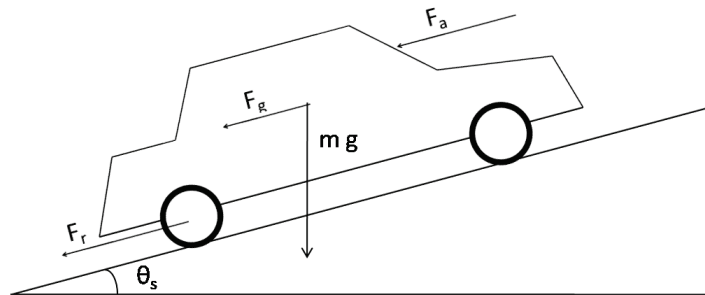


Fig 11 The longitudinal vehicle model

Variables and Constants	
m	Vehicle mass [kg]
g	Gravity acceleration [m/s ²]
θ_s	Road inclination [rad]
ρ_a	Air density [kg/m ³]
C_D	Vehicle drag coefficient [-]
A_f	Vehicle front area [m ²]
V	Vehicle speed [m/s]
f_r	Rolling resistance coefficient [-]
a	Vehicle acceleration [m/s ²]
J_w	Wheel inertia [kgm ²]
r_w	Wheel radius [m]

Force from the road grade

$$F_g = mgsin(\theta_s) \quad (4)$$

Force from the air-resistance

$$F_a = \frac{\rho_a}{2} C_D A_f V^2 \quad (5)$$

Rolling resistance

$$F_r = mgf_r \quad (6)$$

Acceleration force

$$F_{acc} = ma \quad (7)$$

Wheel inertia

$$F_{wi} = a \frac{J_w}{r_w^2} \quad (8)$$

Required Torque at the wheels

$$T_{req} = r_w (F_g + F_a + F_r + F_{acc} + F_{wi}) \quad (9)$$

The forces F_a and F_r is the energy that is lost to propel the vehicle and F_g , F_{acc} , and F_{wi} is energy build-up, stored as potential and kinetic energy. In this thesis a level road is assumed and thus $F_g=0$.

4.2 Component Modeling

4.2.1 Energy Converters

All the energy converters, ICE, ISG and EM, are modeled in the same way.

$$P_{in} = \frac{T_{conv} \omega_{conv}}{\eta_{conv}} \quad (10)$$

- P_{in} is the consumed power [W]
- T_{conv} is the produced torque [Nm]
- ω_{conv} is the rotational speed [rad/s]
- η_{conv} is the efficiency [-]

The efficiencies of the converters are available in look-up tables and are interpolated for the current operating points. The efficiency takes into account all the losses in the converter at that operating point.

Since the EM can be operated both in generator and motor mode the equation becomes

$$P_{EM} = T_{EM} \omega_{EM} \eta_{EM}^{-sign(T_{EM})} \quad (11)$$

4.2.2 Transmission

The basic transmission equations are:

$$P_{in} \eta_{GB} = P_{out} \quad (12)$$

$$P = T\omega \text{ and } \omega_{in} = \omega_{out} \gamma_{GB} \xrightarrow{\text{yields}} T_{in} \gamma_{GB} \eta_{GB} = T_{out} \quad (13)$$

The gear box efficiency, η_{GB} , is used to account for all the losses that occur between the ICE and the wheels (i.e. Gear Box, Final Drive, Differential) and is assumed to be 90%.

4.2.3 Clutch

For simplicity the clutch itself isn't modeled. Instead, to compensate for some of the extra losses during start from standstill, the ICE is assumed to follow a speed profile shaped like a second order function during the time the vehicle speed is below the lowest possible speed where the first gear can be engaged, see Fig 12. This is done to be a simple representation of how the engine speed varies during start from stand still. So instead of modeling the clutch itself the engine speed profile below is designed to compensate for the fact that during start $P_{prod} > P_{dem}$. T_{ICE} is calculated the same way, but during start $\omega_{ICE} > \gamma_{GB} \omega_{wheel}$, following the speed profile below. Other gear shifts are assumed to be instantaneous and without the use of clutch.

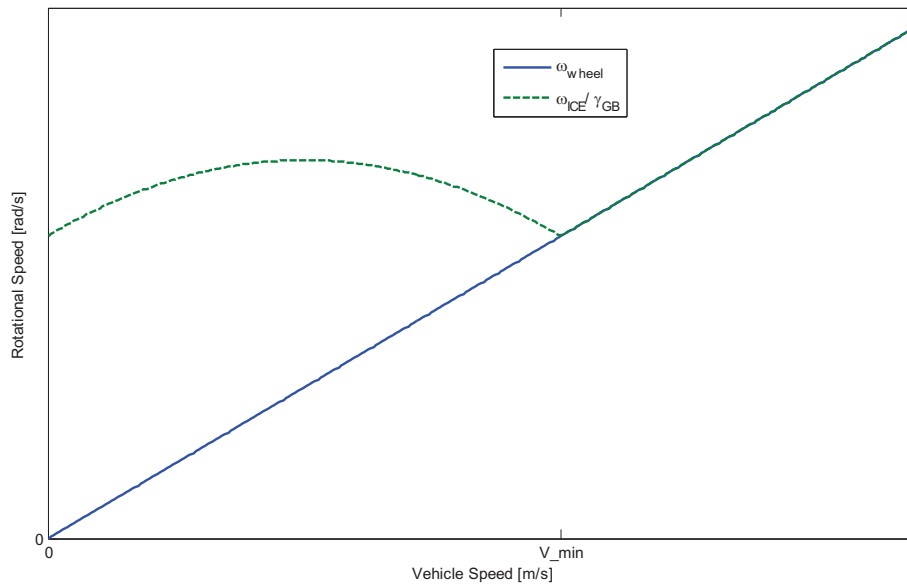


Fig 12 The ICEs speed profile during start from standstill. The speed profile is designed to compensate for the extra losses incurred by the use of a clutch during start. Also in the figure is the corresponding wheel speed profile during start.

4.2.4 Battery

The battery is modeled as an ideal open-circuit voltage source in series with an internal resistance as shown in Fig 13. The battery also supplies the auxiliary units in the vehicle, a power that is assumed constant.

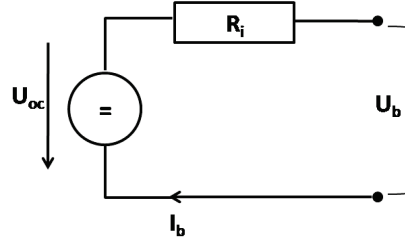


Fig 13 The Equivalent Circuit model of the Battery

According to Kirchoff's Voltage law:

$$U_{oc} - R_i I_b = U_b \quad (14)$$

U_{oc} represents the equilibrium potential of the battery, a quantity that is often considered constant, but normally depends on the SOC. A possible parameterization is:

$$U_{oc} = k_1 SOC + k_2 \quad (15)$$

The power at the battery connection, P_{trm} , can be written as:

$$P_{trm} = I_b U_b \quad (16)$$

(14) with (16) yields:

$$I_b = \frac{U_{oc}}{2R_i} - \sqrt{\left(\frac{U_{oc}}{2R_i}\right)^2 - \frac{P_{trm}}{R_i}} \quad (17)$$

The SOC is defined as the fraction of charge left in the battery.

$$SOC = \frac{Q(t)}{Q_0} \quad (18)$$

Where Q_0 is the battery capacity. The change of charge in the battery can be approximated by the battery current, I_b and the current is considered positive during discharge.

$$\dot{SOC} = -I_b / Q_0 \quad \text{During discharge} \quad (19)$$

$$\dot{SOC} = -\eta_c I_b / Q_0 \quad \text{During Charge} \quad (20)$$

where η_c is the coulombic efficiency that originates from the fact that due to chemical reactions in the battery a fraction of the current isn't turned in to charge.

4.2.4.1 Battery model tuning

The battery parameters were calculated from measured data from the test vehicle, shown in Fig 14. The parameters were calculated with the least squares (LSQ) method. To eliminate some of the distortion on the signals, these were low-pass filtered before the parameter estimation.

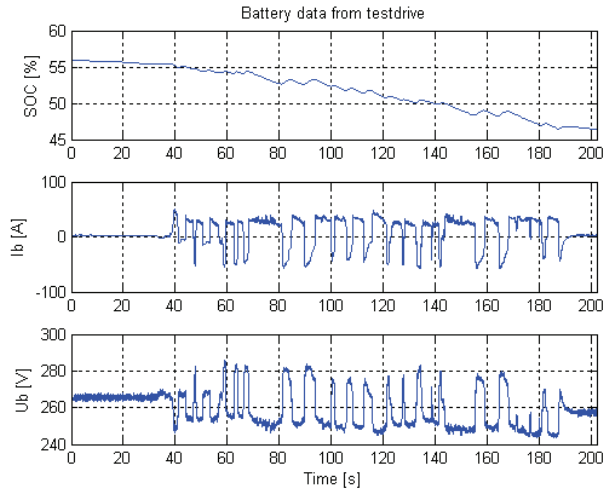


Fig 14 The measured data on which the battery model is validated

First U_{oc} and R_i are estimated as constants according to LSQ and (14). Then U_{oc} as an affine function of SOC was calculated in the same way but using (14) and (15). Below, in Fig 15, is depicted how well the two different models correspond to measured data. The model with $U_{oc}(SOC)$ is a better approximation of the measured data.

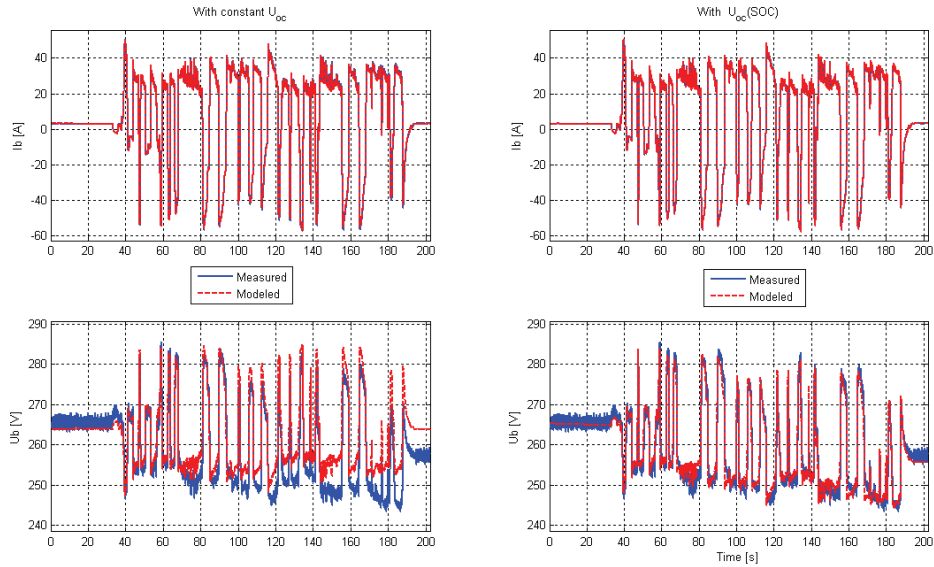


Fig 15 Model performance with constant U_{oc} and $U_{oc}(SOC)$. With constant U_{oc} the error increases with time, resulting in a 10V error after 200s. This is avoided with $U_{oc}(SOC)$

The SOC signal from the battery is discrete and only detects changes that are larger than 1%. Due to this the coulombic efficiency couldn't be calculated with the LSQ method. Instead it is assumed to be a linear function of SOC and then manually tuned to get a good approximation of the measured data. The two different models and their agreement with measured data are shown in Fig 16.

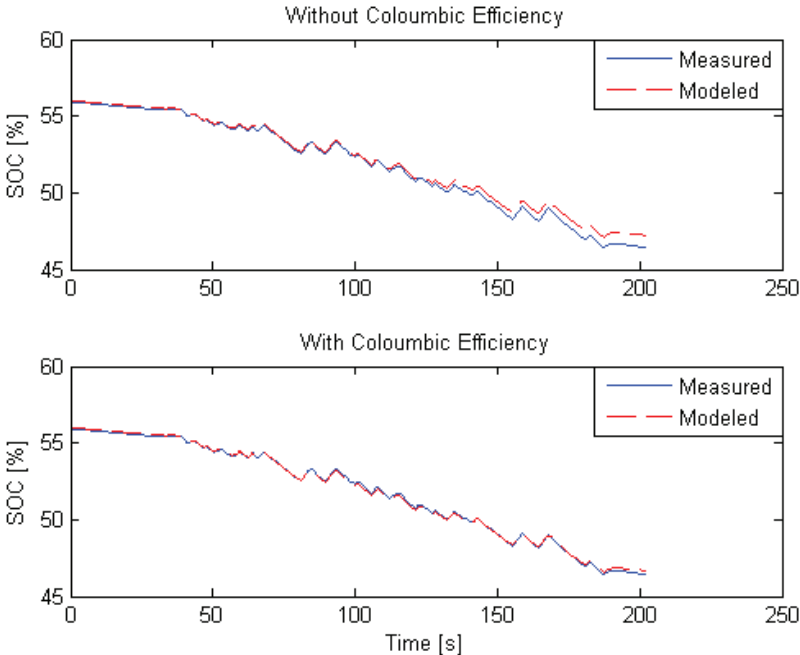


Fig 16 Model performance with and without Coloumbic efficiency.
A constant η_c results in an error that increases with time, thus $\eta_c(\text{SOC})$ is chosen.

In the figures above it is apparent that constant U_{oc} and 100% charge efficiency doesn't suffice to get a good model of the battery. Therefore the full model with $U_{oc}(\text{SOC})$ and $\eta_c(\text{SOC})$ is used.

4.2.5 Powertrain

The vehicle speed is given from the driving cycle, and thus also the possible speeds of the energy converters. The required torque is then calculated from the longitudinal vehicle model. Therefore it suffices to ensure that the combined torque from the converters match the required torque from the drive cycle. The equation becomes:

$$T_{req} = \eta_{GB} \gamma_{GB} (T_{ICE} - \gamma_{ISG} T_{ISG}) + \gamma_{EM} T_{EM} \quad (21)$$

Subject to:

$$T_{EM,min}(\omega_{EM}) \leq T_{EM} \leq T_{EM,max}(\omega_{EM}) \quad (22)$$

$$0 \leq T_{ICE} \leq T_{ICE,max}(\omega_{ICE}) \quad (23)$$

$$0 \leq T_{ISG} \leq T_{ISG,max}(\omega_{ISG}) \quad (24)$$

$$-P_{batt,max}(SOC) \leq P_{batt} \leq P_{batt,max}(SOC) \quad (25)$$

The consumption is calculated as:

$$\dot{m}_f = \frac{\omega_{ICE}(T_{ICE} + J_{ICE} \dot{\omega}_{ICE})}{\eta_{ICE} H_{LHV}} \quad (26)$$

Where $J_{ICE} \dot{\omega}_{ICE}$ is the torque required to accelerate the engine itself.

5 Reference Consumption

To be able to compare the calculated consumptions in the eTVD system using different control strategies, a reference consumption using the eTVD as a conventional AWD vehicle is calculated. This is done using a controller that always selects the gear that results in the lowest fuel consumption for each time-step. The ISG is relay controlled in this mode and it is therefore impossible to control the SOC at the end of the driving cycle, something that is required of the hybrid control. To compensate for this each driving cycle is composed out of 15 repetitions of the same cycle to make the fuel equivalent of the end SOC deviation negligible. The results are shown in Table 1.

Driving Cycle	Consumption
NEDC	6.767 L/100km
FTP-75	6.915 L/100km

Table 1 The consumption of the test vehicle as a conventional AWD vehicle.

6 Dynamic Programming

To find an approximation of the reduction potential available in the hybrid configuration, DDP is used. The algorithm is implemented as described in Section 3.1. The calculations in one iteration of the algorithm are presented below.

6.1 Calculations

To evaluate the cost in fuel to go from one SOC to another at time interval $[t, t+\Delta t]$ the following calculations are performed:

The Current in the battery is calculated from the change in SOC.

$$I_b = \frac{Q_0 \Delta SOC}{\eta_c dt} \quad (27)$$

and the power at the battery connection as a result of the calculated current:

$$P_{trm} = U_{oc} I_b - R_i I_b^2 - DCDC \quad (28)$$

where DCDC is the power needed for the auxiliary system of the vehicle.

The electrical power supplied by the generator:

$$P_{ISG} = T_{ISG} \omega_{ISG} \eta_{ISG} \quad (29)$$

The EM has to supply or accept the produced power from the ISG and battery connection:

$$P_{EM} = P_{ISG} + P_{trm} \xrightarrow{yields} T_{EM} = \frac{P_{ISG} + P_{trm}}{\omega_{EM} \eta_{EM}^{-sign(T_{EM})}} \quad (30)$$

The torque from the ICE is calculated according to:

$$T_{ICE} = \frac{T_{req} - \gamma_{EM} T_{EM}}{\eta_{GB} \gamma_{GB}} + \gamma_{ISG} T_{ISG} \quad (31)$$

All violations of the constraints, (21)-(25) are penalized with a value that in this context symbolizes infinity.

Finally the consumption for that step is calculated according to:

$$\dot{m}_f = \frac{\omega_{ICE} (T_{ICE} + J_{ICE} \dot{\omega}_{ICE})}{\eta_{ICE} H_{LHV}}$$

6.2 Results

Time and SOC are discretized with a step length of 1s and 0.2%. The time discretization is chosen to avoid too long simulations and the SOC discretization is chosen for convenience, since 0.2% roughly equals the change in SOC from the auxiliary units during 1s. The results are shown and discussed in the following sections.

6.2.1 NEDC

The results from the DDP solution are shown in Fig 17-19.

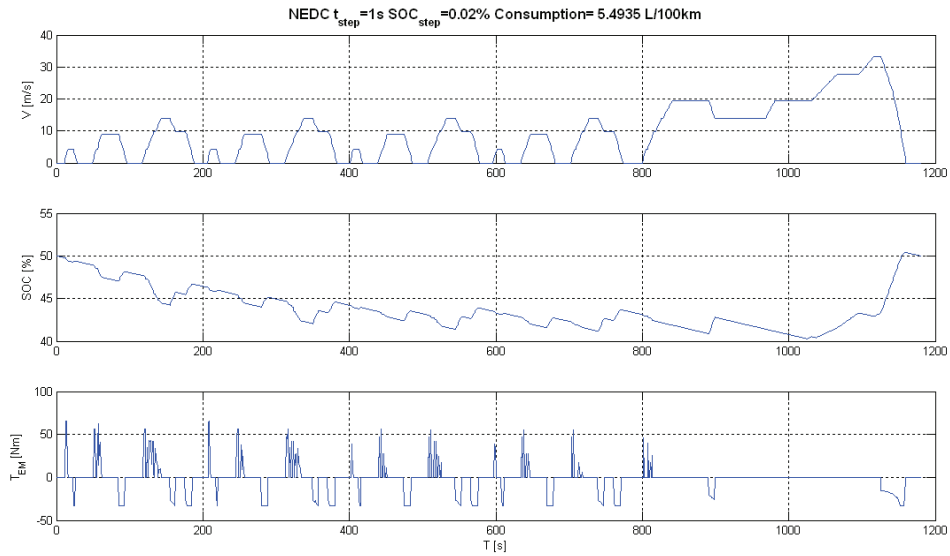


Fig 17 The SOC trajectory and EM usage on the NEDC cycle. The optimal fuel consumption is 5.49 L/100km

As seen in Fig 17 there is a correlation between the SOC and the velocity profile. During accelerations the EM assists the ICE and during decelerations the EM recuperates as much energy as possible. The downward slope of the SOC during the times when the EM isn't in use is due to the power needed for the auxiliary devices.

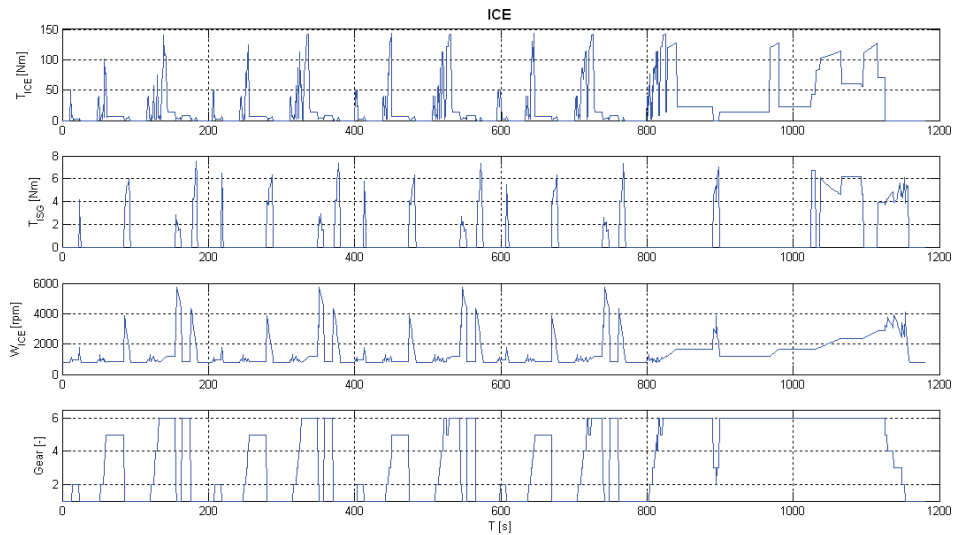


Fig 18 The ICE and ISG usage on the NEDC cycle

Interesting to note in Fig 18 is that the ISG is mainly used during decelerations to recuperate some of the kinetic energy. To maximize the recuperated energy it's also optimal to shift down to a low gear to increase the efficiency of the ISG. The only load shift that occurs is during the last part of the driving cycle, which can be seen in Fig 17, $t \in [1000,1100]$, as the SOC increases even though the vehicle is in traction mode.

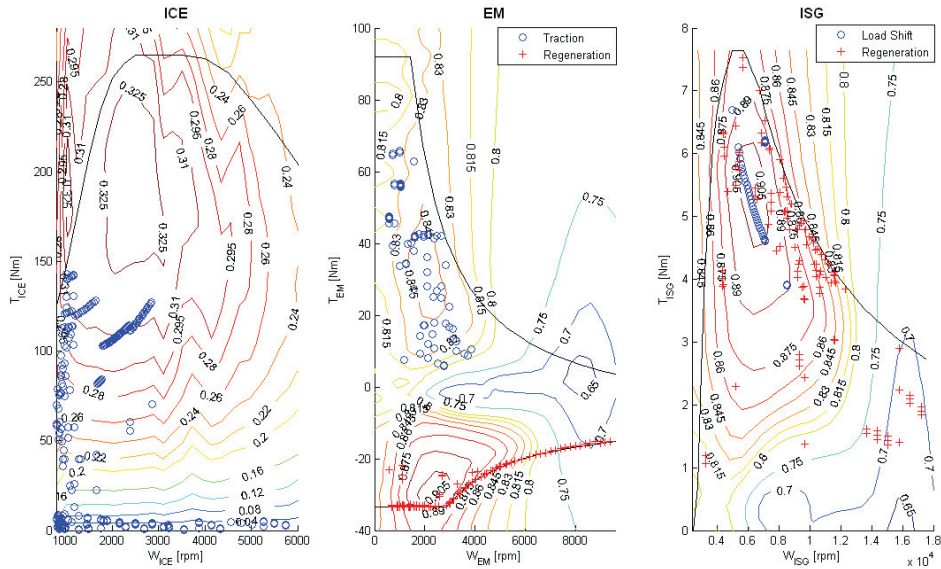


Fig 19 Operating points of the three converters on the NEDC cycle. Noticeable is how the operating points of the EM and ISG are centered around the high efficiency regions when the vehicle is in traction mode.

The operating points, in particular those of the ISG and EM, are mainly in the areas where the converters are the most efficient, see Fig 19. Interesting to note is that almost all the EMs operating points during braking are on, or close, to the torque limit. This is a result of the EM and ISG being designed for torque vectoring and AWD and not as a hybrid. Even with this design optimization the potential for fuel consumption reduction is substantial.

6.2.2 FTP-75

The results from the DDP solution are shown in Fig 20-22.

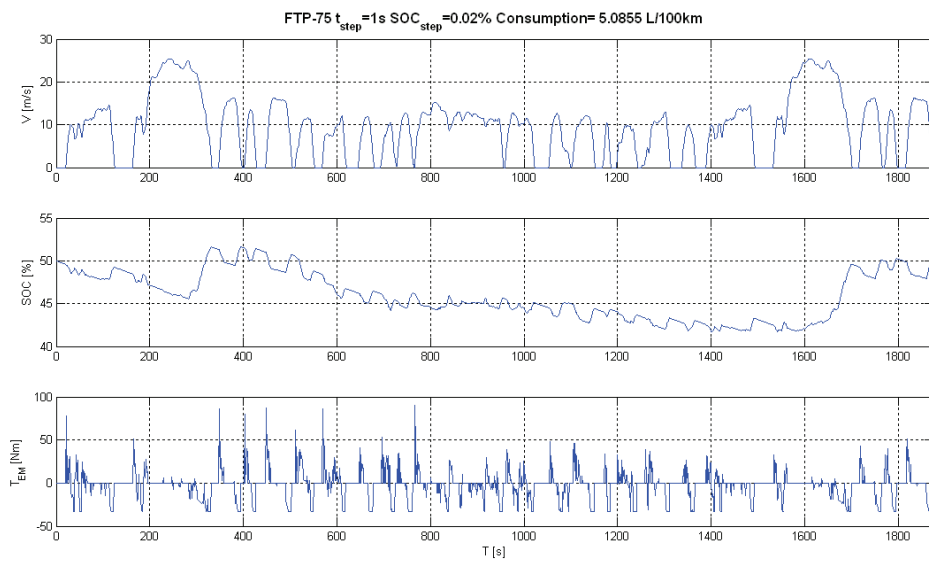


Fig 20 The SOC trajectory and EM usage on the FTP-75 cycle . The optimal fuel consumption is 5.09 L/100km

Compared to the NEDC the FTP-75 appears to be more hybrid-friendly since the consumption as an AWD is higher for FTP-75 than for NEDC, but lower as a hybrid, see Fig 18, 20 and Table 1. This is due to the many starts and stops in the FTP-75 which allows for more energy to be recuperated. It can also be seen by the more extensive EM usage during the FTP-75.

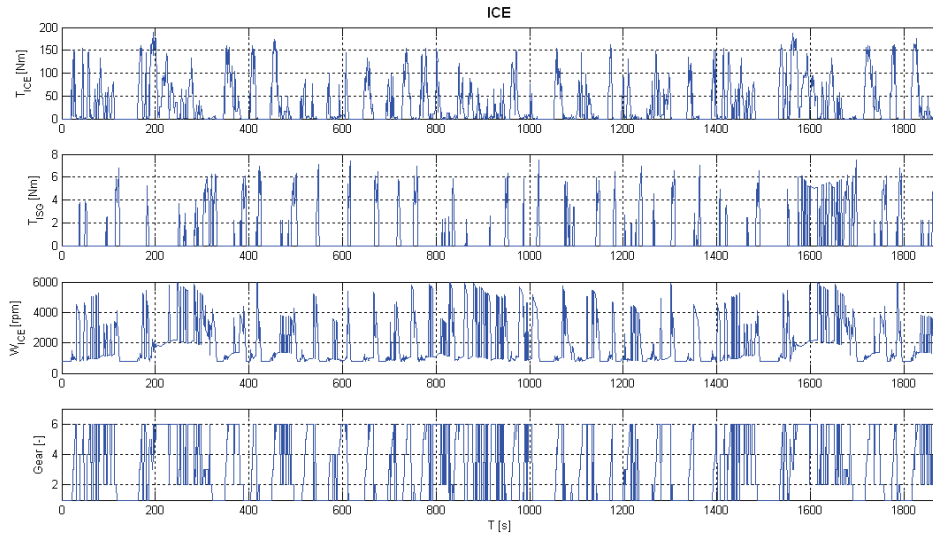


Fig 21 The ICE and ISG usage on the FTP-75 cycle.

Interesting to note in Fig 21 is the many gear shifts that occur during the driving cycle. This is rather unrealistic but since DDP only is an approximation of the minimum consumption it's allowed. As in NEDC the many gear shifts is a result of the systems desire to use the ISG as efficiently as possible.

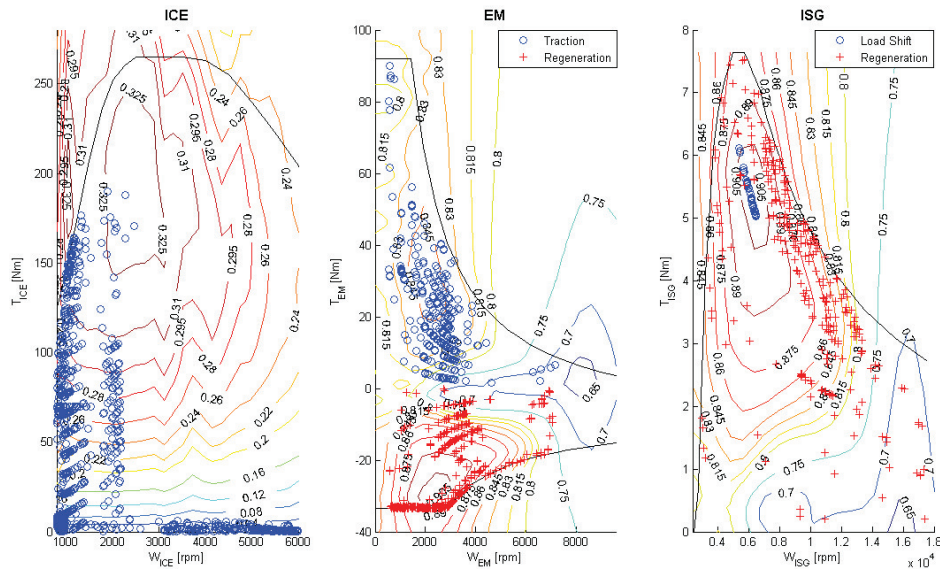


Fig 22 Operating points of the three converters on the FTP-75 cycle As for the NEDC the operating points during traction for the EM and ISG are centered around the high efficiency regions.

As in the NEDC cycle the operating points of the EM and ISG are mainly in the most efficient regions of the converters, see Fig 22. Most of the energy used by the EM is energy that is recuperated during braking. The time spent in load shift is roughly one tenth of the time spent in regenerative braking.

6.2.3 Stability analysis

As mentioned in Section 6.2 the discretization of time and SOC are mainly chosen due to practical considerations. To study how the chosen time and SOC discretizations affect the result of the optimizations a test is carried out on the first part of the NEDC cycle with a different discretization. The ratio between the discretizations is maintained, i.e. one step in SOC still is roughly the same as the change in SOC from the auxiliary units during one time step. The discretizations used are:

- Time step = 1s and SOC step= 0.2‰
- Time step=0.1s and SOC step=0.02‰

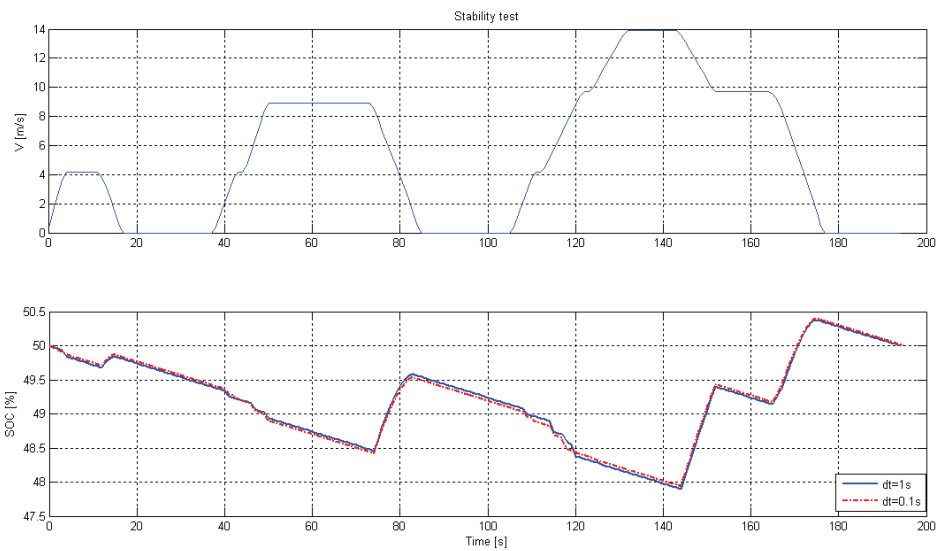


Fig 23 Comparison of the SOC trajectories with different time discretizations on the ECE cycle

As seen in Fig 23 the characteristics of the SOC trajectory remain relatively unaffected by the change in discretization.

Time Step	Consumption
$\Delta t = 1s, \Delta SOC = 0.2\text{‰}$	5.764 L/100km
$\Delta t = 0.1s, \Delta SOC = 0.02\text{‰}$	5.806 L/100km

Table 2 The resulting consumptions on the ECE cycle using different discretizations

The consumption increases slightly as a result of the changed discretization, see Table 2. The reason for this is that with a sparser discretization the required torque to follow the driving cycle becomes more of a mean value model than the actual torque required. This change is however less than 1%, thus the values calculated with a time step of 1s can be considered representative of the reduction potential as a result of hybridization. One could argue that the difference would be larger on a more demanding driving cycle, where more energy could be recuperated and also more is to be gained from using the EM during traction, but since the DDP solution in this thesis only serves as an approximation of the minimum consumption achievable it is neglected.

The optimal consumptions on the two driving cycles calculated in Section 5.2.2 and 5.2.3 are thus considered valid and are shown in Table 3.

Driving Cycle	Consumption	Reduction
NEDC	5.494 L/100km	19%
FTP-75	5.086 L/100km	26%

Table 3 Optimal consumptions on the NEDC and FTP-75 driving cycles and the reduction compared to a vehicle using only AWD.

7 Equivalent Consumption Minimization Strategy

Because of its relative simplicity and the minimum of tuning work needed, the chosen strategy for the real time control system is ECMS with one equivalence factor. As observed earlier this powertrain has two degrees of freedom, not including gear, since the combined torques of the ICE, ISG and EM have to match the required torque, see (21). The solution path for the ECMS calculations is similar to that of the DDP shown in Section 6.1

7.1 Pre-Calculations

Solving (21)-(25) is computationally demanding and therefore the ECMS optimization is performed offline and the result tabulated. In the real-time implementation the control system interpolates in the stored data to find the optimal torque distribution. For the offline calculations the three parameters that the ECMS algorithm takes as input, i.e. vehicle speed, required torque, and equivalence factor, are discretized.

The optimal torque distribution on the three energy converters, as well as the optimal gear, are calculated as a function of (v, T_{req}, λ) for each point. Since, for each gear, it is a two degree of freedom problem it requires two tables for each gear, one for the ISG and one for the ICE. From these two tables the torque required from the EM can be calculated using (21). With six gears, not including reverse, a total of 13 tables are calculated: six ICE, six ISG and one for the gear selection. So the system not only optimizes the torque distribution for the current gear, it also assists the driver in selecting gears by always recommending the gear that would give the lowest fuel consumption. In Fig 24 excerpts from the two tables for the third gear are shown.

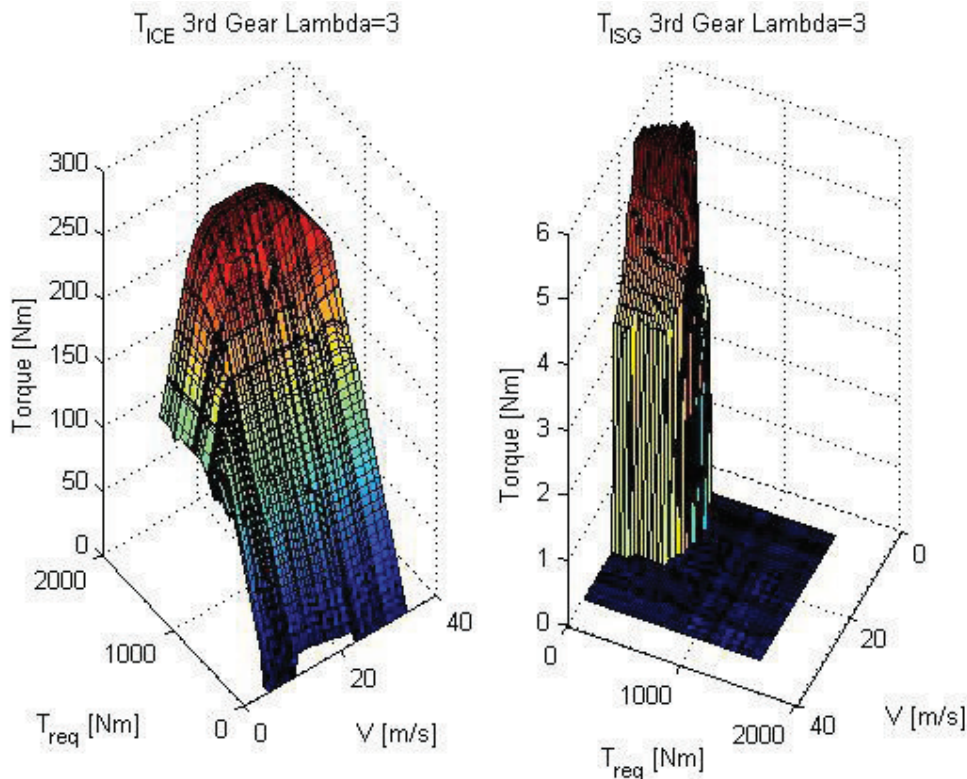


Fig 24 The stored data for the third gear and $\lambda=3$.

In a series production vehicle it is however desirable to keep the memory usage to minimum. Therefore the saved tables shouldn't be larger than necessary. To test how a reduced accuracy, introduced by reducing the size of the tables, affects the consumption, simulations are carried out on two sets of tables, one large set and one small.

To reduce the size in the velocity and torque directions is relatively straight forward even though those points probably should be chosen with care. In the λ direction however, it's a bit harder to visualize which points to include. To get an indication of which points are most important the sum of elements in each table as a function of λ is plotted in Fig 25.

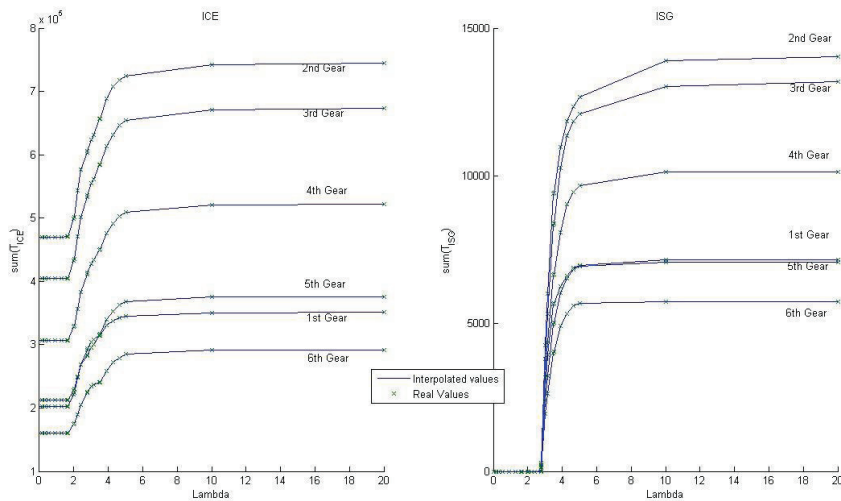


Fig 25 The sum of torque in each table as a function of λ . The left plot is the ICE torque and the right is the ISG.

Since the real-time algorithm uses linear interpolation in the stored data the assumption is that the solution is linear between two optimas. As seen in Fig 25 the change in torque is not linear, but the idea is to make the λ discretization sparser in the segments that could be considered linear and denser where it is clearly non-linear. This is to avoid the loss of too much information. From the figure it is clear that the ISG and ICE tables should have separate λ discretizations. The ISG tables remain constant up until $\lambda \approx 3$ while the ICE tables only remain constant until $\lambda \approx 2$.

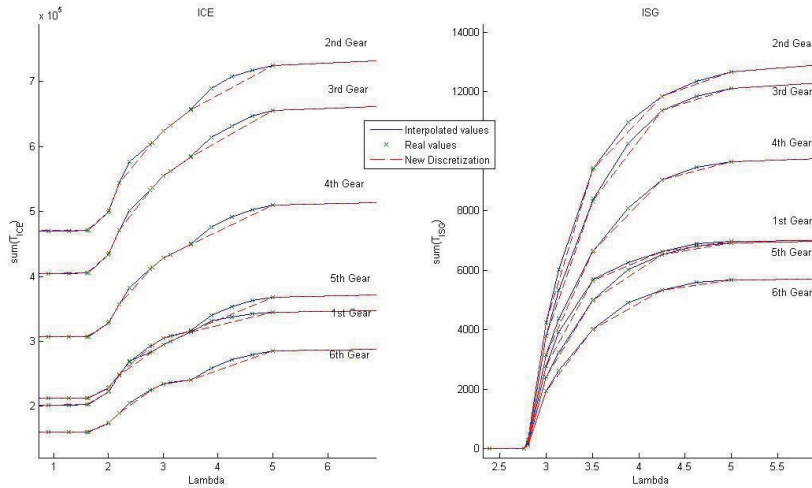


Fig 26 The sum of torque in each table as a function of λ with the original as well as the new discretization.

In Fig 26 it is shown how well the new discretization approximates the old discretization. It's apparent that information will be lost when making the discretization sparser. This is since it's clear that the sum of the stored torque does not behave linearly when λ change. In Fig 27 the same excerpt as in Fig 24 is shown, but with the new discretization. The result of making the discretization sparser in all three directions is a set of tables eight times smaller than the original set.

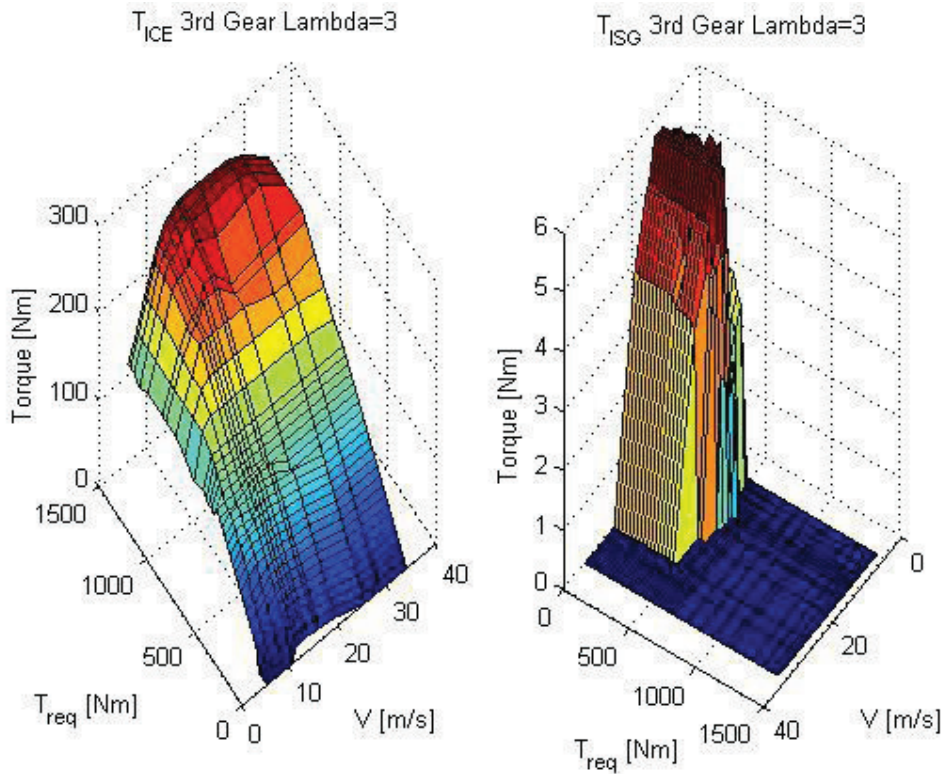


Fig 27 The tables after the grid is made sparser

7.2 Implementation

The system that is implemented consists of three blocks.

- λ : A block that takes the battery signals as input and the output is the value of the adjoint state, λ .
- Gear selector: A block that takes the vehicle speed and required torque as inputs and the gear that should be engaged at that moment is the output.
- ECMS: The block that performs the torque distribution.

7.2.1 The Gear Selector

The gear selector consists of one look-up table where the optimal gears from the offline calculations are stored. But since the result is produced with interpolation there is no guarantee that the recommended gear is valid. For instance close to the speed where the second gear can be engaged the interpolation might suggest gear 1.8 which is rounded to 2. But to engage the second gear at such a point would lead to undesired performance. Therefore the recommendation is limited to those gears that might actually be engaged at that time.

To prevent too frequent gear shifts a hysteresis of 10% is applied on the gear selection. For example, to change from 4th to 3rd gear the result of the interpolation has to be 3.45 or lower and to go from 3rd to 4th it has to be 3.55 or higher.

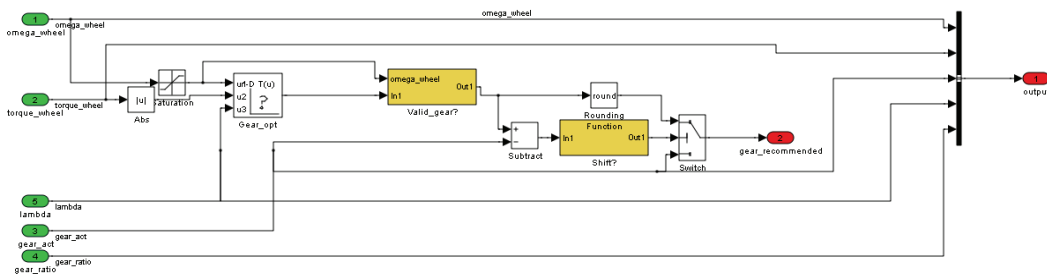


Fig 28 The Gear Selector Block

Since the test vehicle has a manual gear box the Gear Selector can only recommend which gear the driver should engage. In simulations the system follows the Gear Selector and shifts instantaneous without the use of a clutch, as described in Section 4.2.3.

7.2.2 The ECMS block

The ECMS block consists of two main systems, aptly named Throttle and Brake. In this implementation it's only the Throttle block that actually uses the ECMS strategy. The main reasons behind this separation are that it is unclear whether the braking could be controlled in the test vehicle and because the main variable that affects the possibility to recuperate energy is the gear selection. It is assumed that the time spent in braking is so short that an extra gear shift would be impractical. Therefore to reduce the memory usage, only positive required torque is stored.

So instead the brake block brakes as much as possible with the EM and if the magnitude of required negative torque is greater than what the EM can produce, the ISG is used as well.

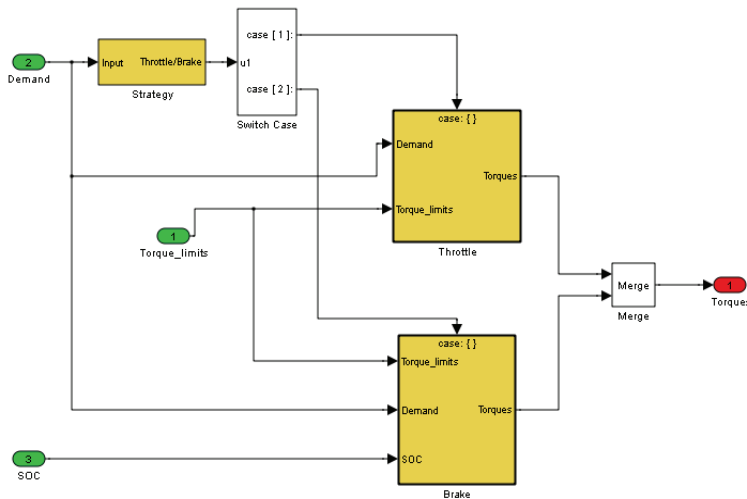


Fig 29 Overview of the ECMS block

The Throttle block consists of six similar blocks, one for each gear, that interpolate to find the torque distribution on the ICE and ISG. Another block then limits the torques so they don't violate any constraints and calculates the torque on the EM according to (21).

7.3 Simulation Results

During the simulations a λ is considered optimal if the end SOC is the same as the start SOC. To find the optimal λ a trial and error iterative approach is used. All simulations are carried out with a time step of 0.1s.

7.3.1 Analysis and Interpretation of NEDC Results

Cycle	Performance	Small tables	Large tables	DDP	AWD
NEDC	λ_{opt}	2.8448	2.8247	-	-
	Consumption	5.711 L/100km	5.707 L/100km	5.494 L/100km	6.767 L/100km
	Reduction	15.6%	15.7%	19%	-

Table 4 The Optimal λ and associated consumption with the small and large sets of tables on the NEDC cycle. For comparison the consumption from DDP as well as the consumption as a strictly AWD vehicle is included

The resulting consumption and optimal λ for simulations using both small and large tables are given in Table 4. The higher λ and consumption for the small tables is a result of information being lost when the tables are made smaller. To study this further the SOC trajectories for small and large tables as well as Dynamic Programming is displayed in Fig 30.

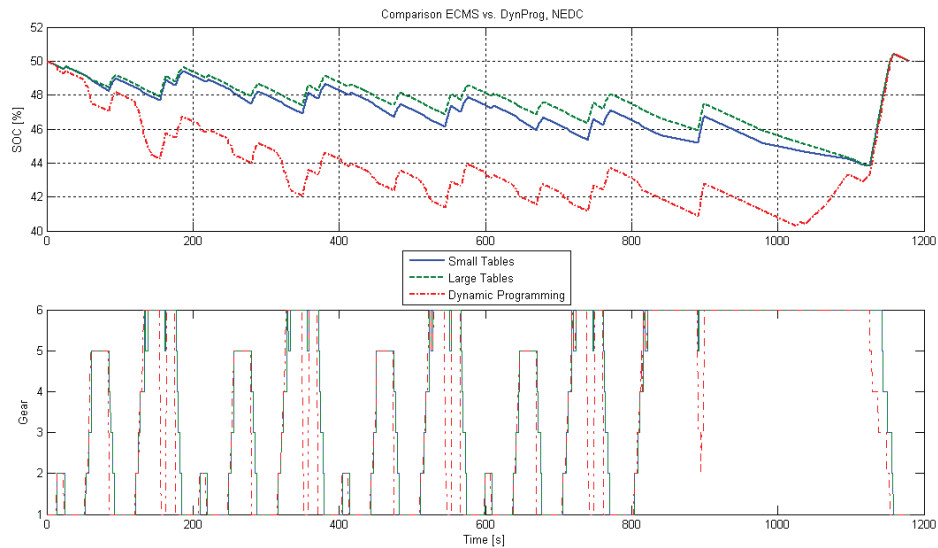


Fig 30 The SOC trajectories and the selected gears with small and large tables as well as with DDP on the NEDC cycle.

In Fig 30 it's visible that the performance of the system changes when smaller tables are used. The characteristics of the ECMS solution resemble that of DDP but since the ECMS uses interpolated values it loses some of the optimality. One interesting thing to note is that the SOC trajectory with small tables is closer to that of DDP than the trajectory of the simulation with large tables.

Since the ECMS algorithm doesn't handle braking it cannot shift gear to use the ISG in a more efficient way. This limits how much energy that can be recuperated and thus the ECMS cannot use as much of the battery as DDP. Using less of the battery capacity may be sub-optimal in a consumption perspective but it reduces the wear on the battery, which is an important factor in a real implementation.

To see how the operating points change between small and large tables the operating points of the two are plotted below, small in Fig 31 and large in Fig 32.

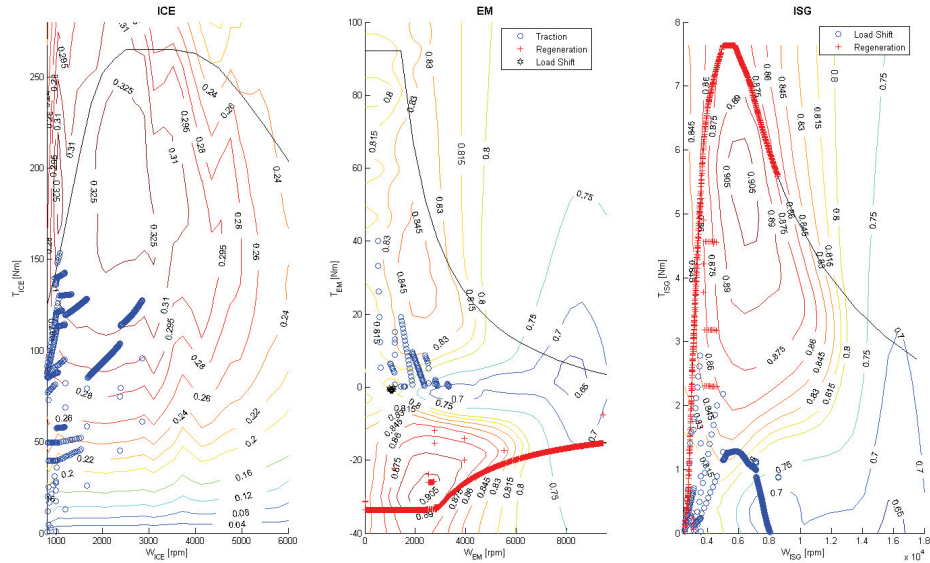


Fig 31 Operating points of the ECMS algorithm on the NEDC cycle using small tables. The ECMS solution doesn't use the EM and ISG in a particularly efficient way. Even the EM is being used to load shift, see plot 2 around 1000rpm and 0Nm.

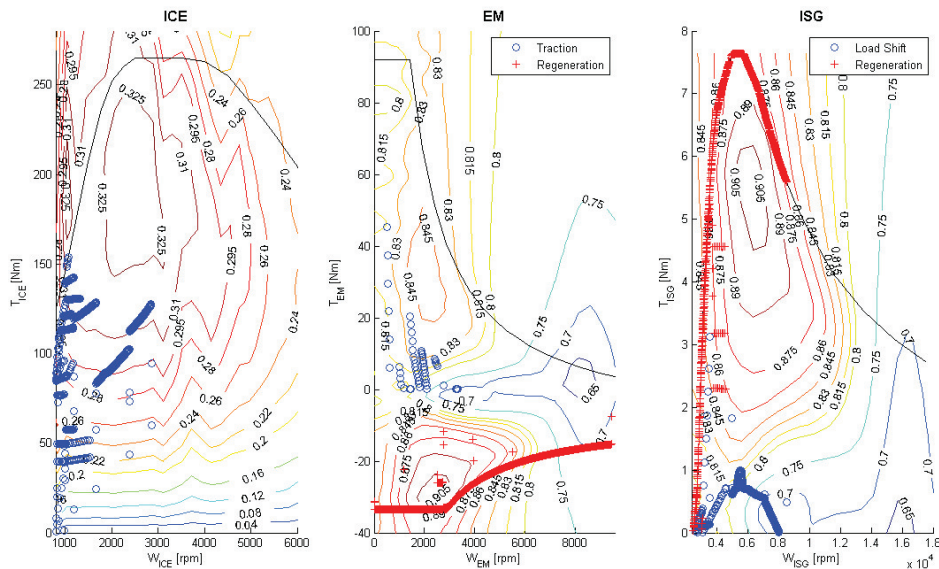


Fig 32 Operating points of the ECMS algorithm on the NEDC cycle using large tables. The ECMS solution doesn't use the EM and ISG in a particularly efficient way

Comparing Fig 31 and Fig 32 it's seen that the small tables uses the EM in traction more than the large but to compensate for this the system load shifts more. As seen in Fig 31 it even uses the EM to load shift. This is most likely, since the torque on the wheels from the ICE exceeds the required torque from the driving cycle. Also the EM and ISG aren't used in a particularly efficient way. Whereas the

operating points of the DDP solution, see Fig 19, were mainly in the high efficiency regions, the ECMS doesn't show such characteristics.

7.3.2 Analysis and Interpretation of FTP-75 Results

Cycle	Performance	Small tables	Large tables	DDP	AWD
FTP-75	λ_{opt}	2.71775	2.66415	-	-
	Consumption	5.470 L/100km	5.458 L/100km	5.086 L/100km	6.915 L/100km
	Reduction	20.9%	21.1%	26%	-

Table 5 The Optimal λ and associated consumption with small and large tables on the FTP-75 cycle. For comparison the consumption from DDP as well as the consumption as a strictly AWD vehicle is included

The consumption on the FTP-75 cycle follows the result already discussed on the NEDC, small tables result in a slight increase in the consumption due to the precision loss by making the discretization sparser. In Fig 33 the SOC trajectories of the two different sets of tables as well as the DDP solution are shown.

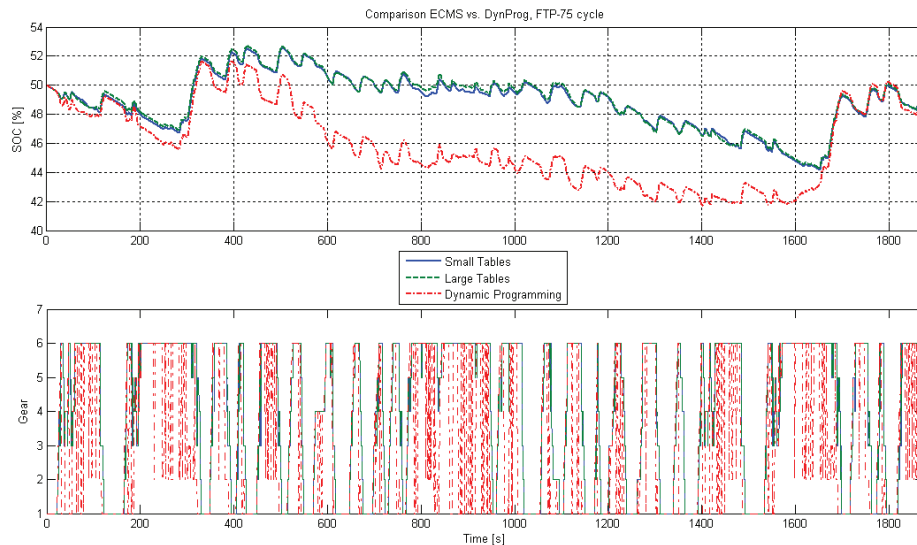


Fig 33 The SOC trajectories and the selected gears with small and large tables as well as with DDP on the FTP-75 cycle

As seen in Fig 33 the SOC trajectories for the two sets of tables are very similar to each other, but they differ from the trajectory from DDP. The ECMS simply can not recuperate as much energy as the DDP since it does not control the braking and has no knowledge of the driving cycle, other than the equivalence factor λ . To study the difference between the two sets of tables the operating points are shown in Fig 34, small tables, and Fig 35, large tables.

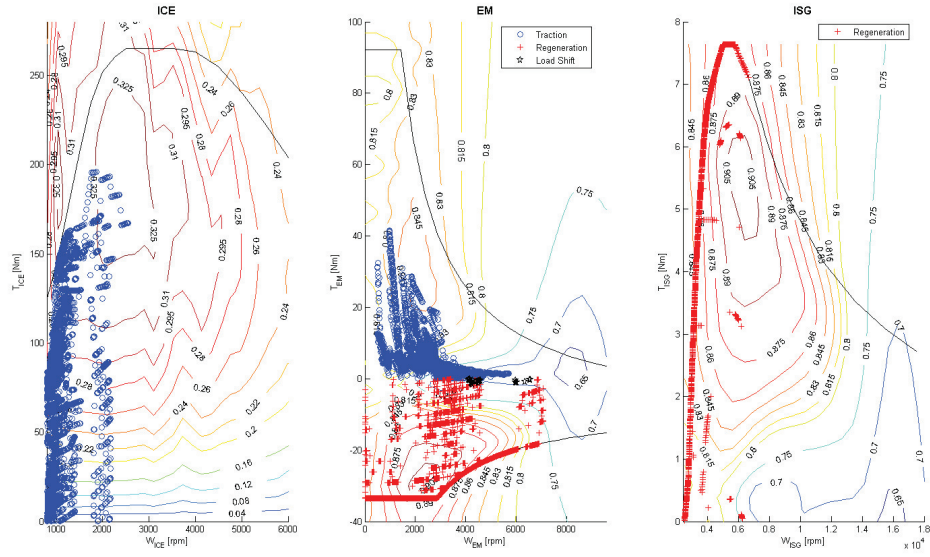


Fig 34 Operating points of the ECMS algorithm on the FTP-75 cycle using small tables. The ISG is never used in load shift but the EM is, see plot 2 around 4000 and 6000rpm and 0Nm.

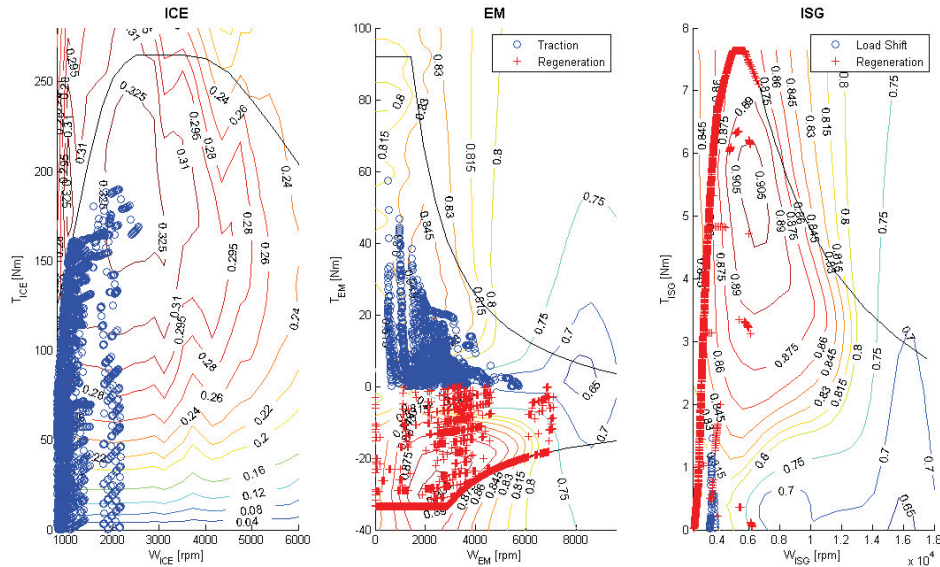


Fig 35 Operating points of the ECMS algorithm on the FTP-75 cycle using large tables.

The results for FTP-75 are in line with the results from the NEDC simulations, see Fig 34-35. The large tables utilize the EM and ISG in a more optimal way than the small tables, hence the slightly lower consumption. Interesting to note is that the small tables doesn't use the ISG, but the EM, in load shift, see Fig 34. This is most likely a symptom of information being lost in the smaller tables, since the extra losses induced by the gear box (and tires in reality) should make the system favor the ISG over the EM in load shift; which is also the case in the DDP and large table solutions.

7.3.3 ECMS evaluation

The results of the simulations with optimal λ for the two driving cycles are summarized in Table 6.

Cycle	Performance	Small tables	Large tables	DDP	AWD
NEDC	λ_{opt}	2.8448	2.8247	-	-
	Consumption	5.711 L/100km	5.707 L/100km	5.494 L/100km	6.767 L/100km
	Reduction	15.6%	15.7%	19%	-
FTP-75	λ_{opt}	2.71775	2.66415	-	-
	Consumption	5.470 L/100km	5.458 L/100km	5.086 L/100km	6.915 L/100km
	Reduction	20.9%	21.1%	26%	-

Table 6 The optimal λ and the associated consumption for different driving cycles.

The ECMS simulations show that ECMS produce a good result on a given driving cycle, close to that of DDP, with both small and large tables. However the usage of the converters differs between the two optimization strategies. This is probably due to the fact that the ECMS implementation uses interpolated values assuming a linear relation between different equivalence factors, which clearly is not the case (see Fig 25-26). One problem is that if for instance $T_{ISG}(\lambda_1)=0\text{Nm}$ and $T_{ISG}(\lambda_2)=8\text{Nm}$ then $T_{ISG}(\lambda_1 < \lambda < \lambda_2)$ will be somewhere between 0Nm and 8Nm disregarding the efficiencies of the converters at that operating point.

7.4 Prediction of the Equivalence Factor

Even if the simulations show that the implemented ECMS produce a good result on a given driving cycle, close to that of DDP, it is also seen that the optimal values of λ are very specific and the system seems to be quite sensitive. An optimal λ from one driving cycle is not necessarily charge sustaining on another, see Fig 36.

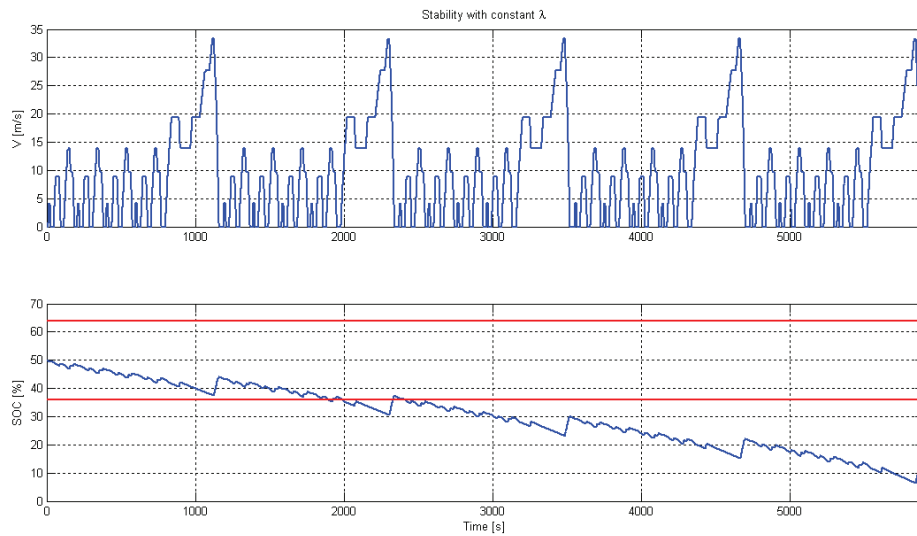


Fig 36 The NEDC cycle repeated five times with the optimal λ from the FTP-75 cycle.

The controller has to adapt to the driving scenario. Since the test vehicle lacks equipment to assess the future driving mission the equivalence factor has to adapt based only on the past and present driving conditions. The state used for adaptation is the battery SOC. Under the assumption, from Section 3.2.3, that there exists one λ that approximates a given driving cycle, the controller should

ideally find that λ for the future driving mission and use that value for the entire mission. Since this is not possible without predicting the future a different approach is devised.

7.4.1 Static Prediction based on SOC

To allow the system to use as much of the battery capacity as possible the idea is to create a function that is flat around the center of the desired SOC window. However, when the SOC approaches the limits of the SOC window it needs to adapt to ensure charge sustenance. The chosen function that fulfills these requirements is a tangens function, see Fig 37.

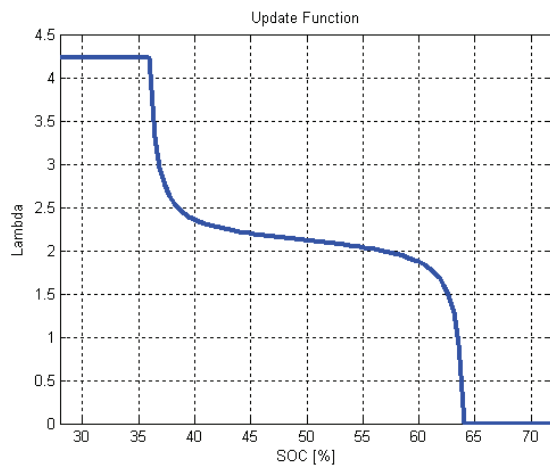


Fig 37 The Update function is a tangens function that is scaled so the smallest gradient (center) is at the center of the SOC window and at the λ that approximates the driving cycle. The horizontal parts of the function are outside the desired SOC window.

At each time λ is decided from $\lambda = f(\text{SOC})$ where $f(\text{SOC})$ is a tangens function as shown in Fig 37. Clearly the slope of the function around the center is a design parameter. To study how the slope affects the performance of the system, the optimal SOC trajectories for different slopes are plotted in Fig 38.

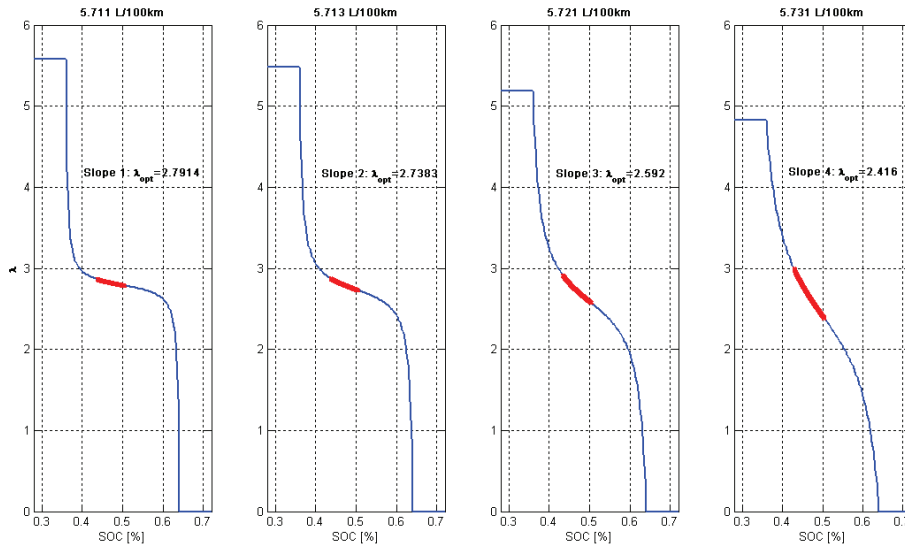


Fig 38 The SOC trajectory and consumption for different slopes on the NEDC cycle. The consumption increases with the slope

As seen in Fig 38 the consumption increases with the slope. One could also assume that the ability of the system to keep the SOC within the desired SOC window, increases with the slope, since a change in SOC then results in a larger change in λ . To study this, simulations are done of the NEDC cycle with intentional wrong initial λ values and different slopes of the tangens function. The results are shown in Fig 39.

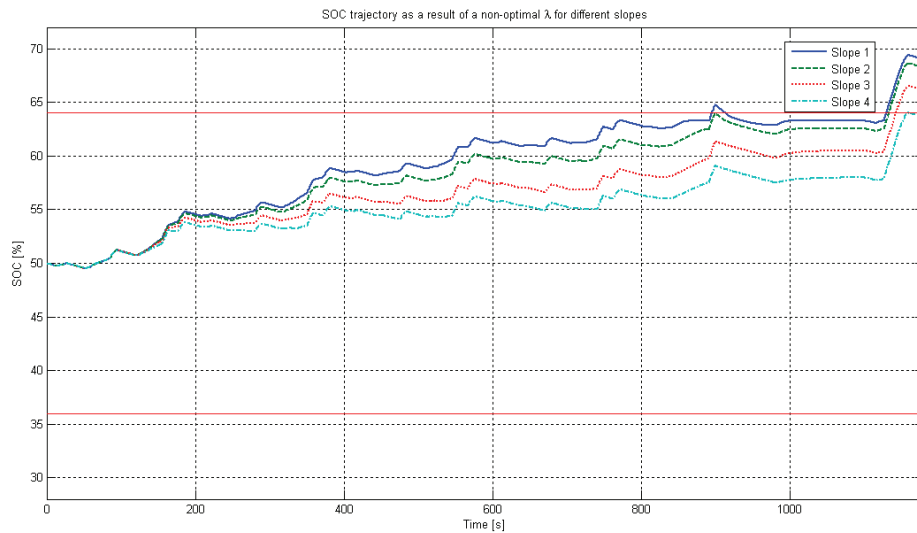


Fig 39 SOC trajectories for different slopes, NEDC cycle and $\lambda=4$. The plot confirms the previous theory that a steeper slope is more robust but it also shows that a steep slope alone doesn't guarantee that the SOC stays within the desired SOC window.

The previous assumption, that a slope increase increases the ability to maintain the SOC within the SOC window is correct. However, since there is no way of knowing the optimal λ for the current

driving mission there is no slope that alone guarantees charge sustenance. So the choice is a trade-off between charge sustenance and fuel consumption. Here Slope 2 is chosen. In Fig 40 the same test as in Fig 36 is shown, now with the use of Static Prediction based on SOC (SP).

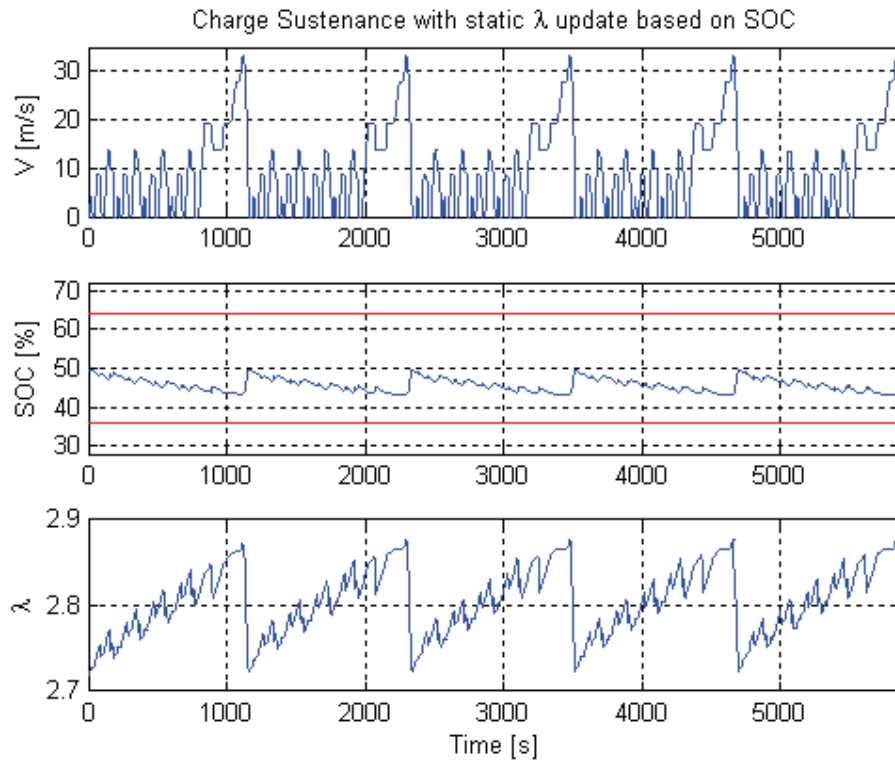


Fig 40 The NEDC cycle repeated five times with the optimal λ from the FTP-75 cycle and Static Prediction based on SOC. The system is now capable of maintaining the SOC within the desired SOC window despite a non-optimal λ

With the use of the new adaptation the system is not as sensitive to the initial λ . The system is charge sustaining despite the use of the optimal λ from the FTP-75 cycle.

7.4.2 Results with Static Prediction based on SOC

The resulting consumptions with the two different sets of tables and the devised adaptation are shown in Table 7.

Driving Cycle	Performance	Small tables	Large tables
NEDC	$\lambda_{opt,init}$	2.7383	2.7301
	Consumption	5.713 L/100km	5.708 L/100km
	Reduction	15.58%	15.65%
FTP-75	$\lambda_{opt,init}$	2.68544	2.6403
	Consumption	5.470 L/100km	5.458 L/100km
	Reduction	20.9%	21.1%

Table 7 The optimal λ and the associated consumption for different driving cycles with the use of SP. Also included is the consumption reduction compared to the strictly AWD vehicle

Observe that the λ that approximates the driving cycle changes when SP used. Also visible is that the use of SP only results in a slight increase in the consumption, see Table 6.

7.4.3 Adaptive Prediction based on SOC

The proposed strategy has introduced some adaptivity to the system, but since there is no way of knowing the λ that approximates the future driving mission, it is not necessarily enough. The initial value of λ is still important. As seen in Fig 41 the SOC doesn't stay within the SOC window when the initial value differs too much from the value that actually approximates the driving cycle.

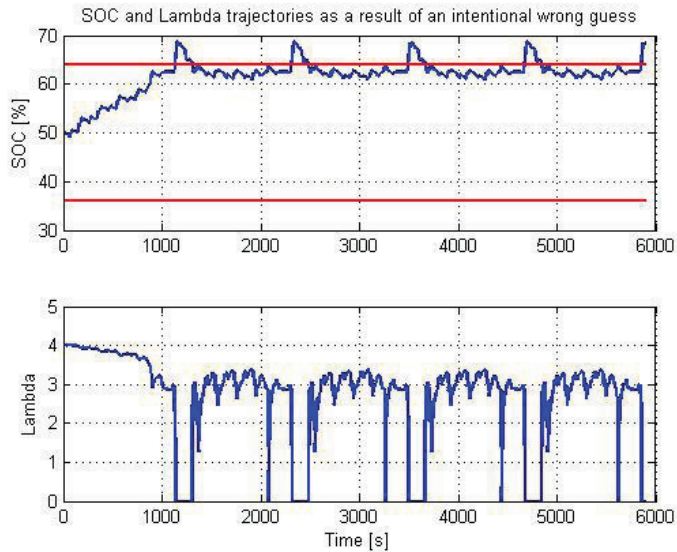


Fig 41 The SOC and λ trajectories during a wrong guess. NEDC cycle repeated five times, small tables. Initial value of $\lambda=4$. The system starts to oscillate around a SOC value that is not necessarily within the desired SOC window.

Instead the system instead starts to oscillate around a SOC value that is not necessarily within the SOC window. The corresponding λ value seems to oscillate around a value close to the $\lambda_{opt,init}$ found in Table 7. The idea is thus to let the center of the function proposed in Section 7.4.1 change according to the trend of the λ values. To find the trend a low-pass filter is used. For this the time constant of the filter needs to be chosen. In Figure 42 and 43 the characteristics with the use of different low-pass filters are shown.

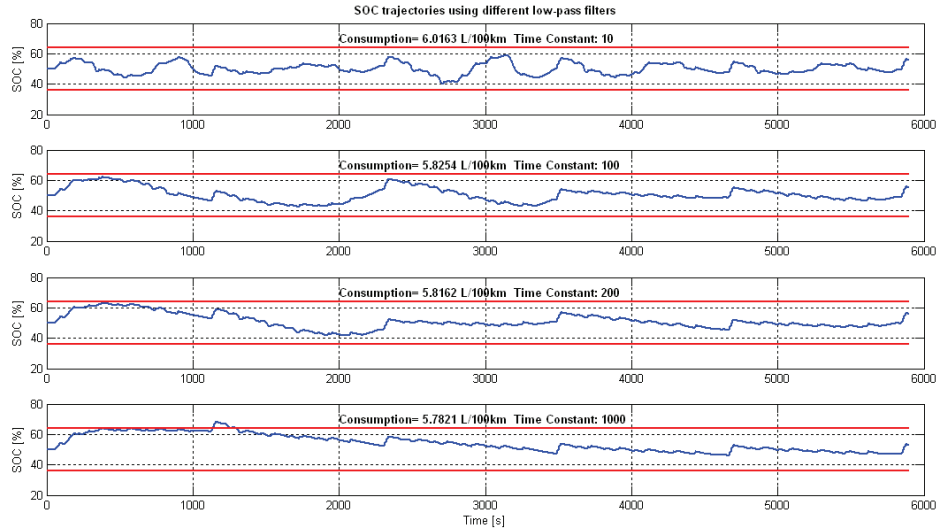


Fig 42 The SOC trajectory with the use of different low-pass filters. Initial $\lambda=5$, NEDC cycle repeated five times.

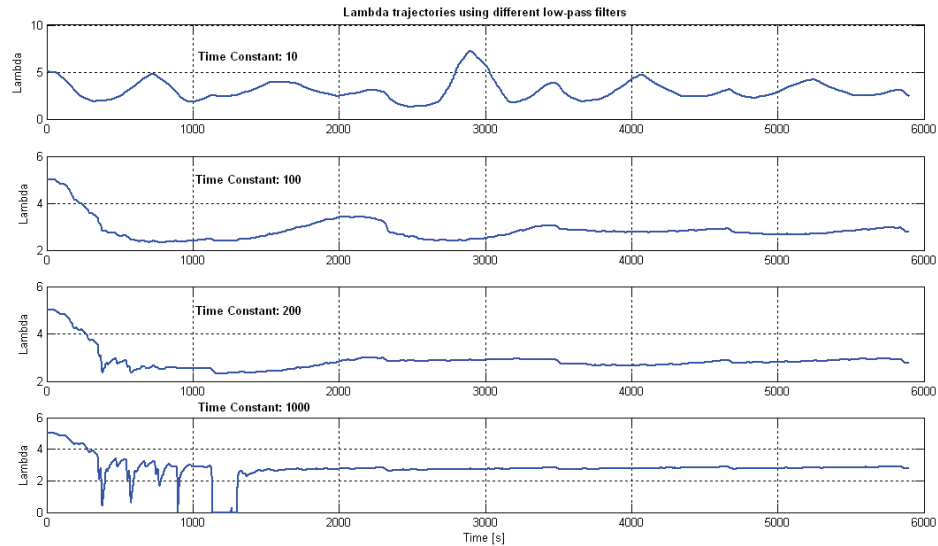


Fig 43 The λ trajectory with the use of different low-pass filters. Initial $\lambda=5$, NEDC cycle repeated five times.

The trade-off is between system speed and fuel consumption, see Figures 42 and 43. If the time constant is small, the system will find the optimal λ region fast, in this case decrease from 5 to 2.74. But a fast filter also means that the center of the tangens function becomes sensitive to the current λ which gives an oscillative system that increases the fuel consumption. Looking at Figures 42 and 43 it is apparent that the time constant should be in the 100-200s region. Here 200s is chosen.

In order to evaluate the charge sustenance of the control with Adaptive Prediction based on SOC (AP) it is tested in Haldex Vehicle Simulator (VehSim). The VehSim is a software that makes it possible to test different controllers without having to implement them in a real vehicle. The vehicle in VehSim is controlled by a driver using the same controls as in a vehicle, i.e. steering-wheel, accelerator, brake and clutch.

The test consists of three phases. The first and last phases consist of very aggressive driving, forcing the EM to assist the ICE in traction. The second phase tries to emulate ECO-driving. The results are shown in Fig 44.

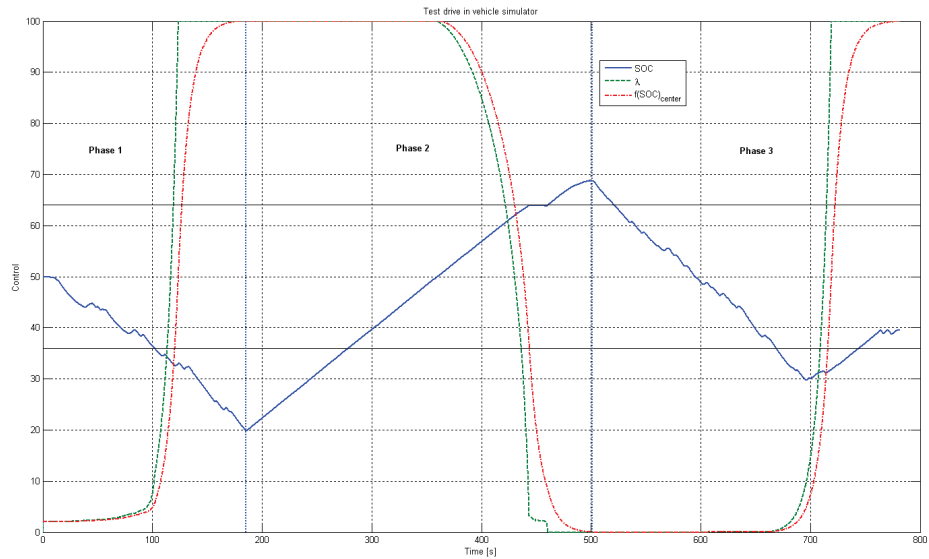


Fig 44 The λ , $f(\text{SOC})_{\text{center}}$ and SOC trajectories during a test in a vehicle simulator

As seen in Fig 44 the control doesn't manage to maintain the SOC within the desired SOC window. During phase 1 both λ and the center of the tangens reach their limits. Because the filter is slow the system doesn't manage to get λ and the center of the tangens function down to the normal operating region during phase 2. The build-up brought on by the aggressive driving causes the AP to oscillate between its end values, similar to integral windup in a normal PID-controller. To prevent this the possible values of the tangens center are limited so that it only operates in what can be considered a feasible region, chosen to be between 2 and 6.

7.5 System performance on unknown cycles

Since the driving mission almost always is unknown it's desirable to test how the system acts when the driving cycle is different from the driving cycles for which it is designed. To simulate this six driving cycles are used. The driving cycles are:

- Hyzem Urban
- Hyzem Rural
- EPA Highway Fuel Economy Test Cycle
- The US06 Supplemental Federal Test Procedure

Because the speed in the US06 cycle is higher than the desired max speed of the test vehicle the velocity points are scaled with 0.9.

- New European Driving Cycle
- Federal Test Procedure-75

To simulate real driving these cycles are selected at random to create a driving mission 30 driving cycles long on which the systems are tested. The 30 selected driving cycles represent roughly 8 hours of driving and a distance of 350km.

On this driving mission the ECMS with both adaptive and static prediction based on SOC is tested with both small and large tables.

7.5.1 The ECMS with Static Prediction based on SOC

The results of the simulation with SP and small and large tables on the driving cycle described in Section 7.5 are shown in Fig 45.

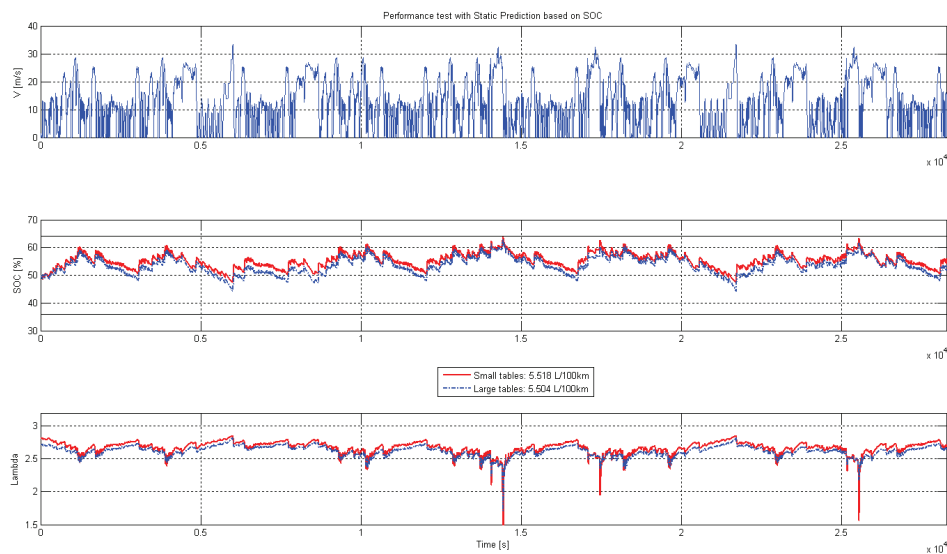


Fig 45 Performance test with Static Prediction based on SOC. The system is charge sustaining over the randomized driving cycles and the small tables result in a slightly higher consumption than the large tables.

As seen in Fig 45 the system is charge sustaining on the randomized driving cycle, since the SOC is always within the SOC window. The consumptions are also in line with the previous results and the system with the small tables has a slightly higher consumption than the system with large tables. Due to the length of the driving mission the difference in end SOC is negligible.

7.5.2 The ECMS with Adaptive Prediction based on SOC

The results of the simulation with AP and small and large tables on the driving cycle described in Section 7.5 are shown in Fig 46.

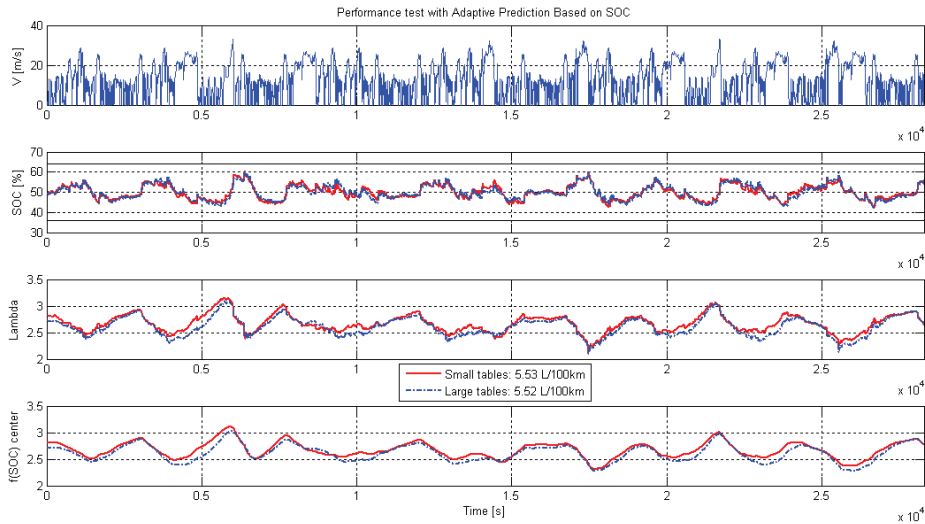


Fig 46 Performance test with Adaptive Prediction based on SOC. The system is charge sustaining over the randomized driving mission and the small tables result in a slightly higher consumption than the large tables.

As seen in Fig 46 the system with AP is also charge sustaining on the randomized driving cycle with fuel consumption in line with earlier test results.

7.5.3 Evaluation

The same driving mission as described in Section 7.5 is also carried out as a strictly AWD vehicle, as described in Chapter 5, to be able to compare the hybrid systems. The results are presented in Table 8.

Configuration	Tables	Consumption	Reduction
AWD	-	6.673 L/100km	-
ECMS w. SP	Small	5.52 L/100km	17.3%
	Large	5.50 L/100km	17.6%
ECMS w. AP	Small	5.53 L/100km	17.1%
	Large	5.52 L/100km	17.3%

Table 8 The results of the performance tests.

The AP increases the consumption of the system, but as seen in previous sections it also increases the ability of the system to maintain the SOC within the SOC window. However, as seen in Section 7.5.1, in normal driving situations this extra robustness is unnecessary since the system with SP also ensures charge sustenance during a set of random driving cycles.

8 Vehicle Tests

The system that is chosen to be implemented in the test vehicle is the one with small tables and Adaptive Prediction based on SOC. The small tables are chosen because of the substantial decrease in memory usage and only slight increase in fuel consumption. Even though it was shown in Section 7.5.1 that AP is not necessary under normal driving circumstances the extra robustness of the AP is considered desirable. The two test drives, see Figures 47-50, try to represent urban driving with many transients and low speed and are done to test the driveability and the charge sustenance of the control system. The first test drive, see Figures 47 and 48, is done with normal SOC but a high λ_{init} and the second test drive, see Figures 49 and 50, is with normal λ_{init} and high SOC.

The torques T_{rear} and T_{front} is the torques on the front and rear axis respectively.

$T_{front} = \eta_{GB} \gamma_{GB} (T_{ICE} - \gamma_{ISG} T_{ISG})$ and $T_{rear} = \gamma_{EM} T_{EM}$ where T_{rear} is considered positive in propulsion and negative in regeneration.

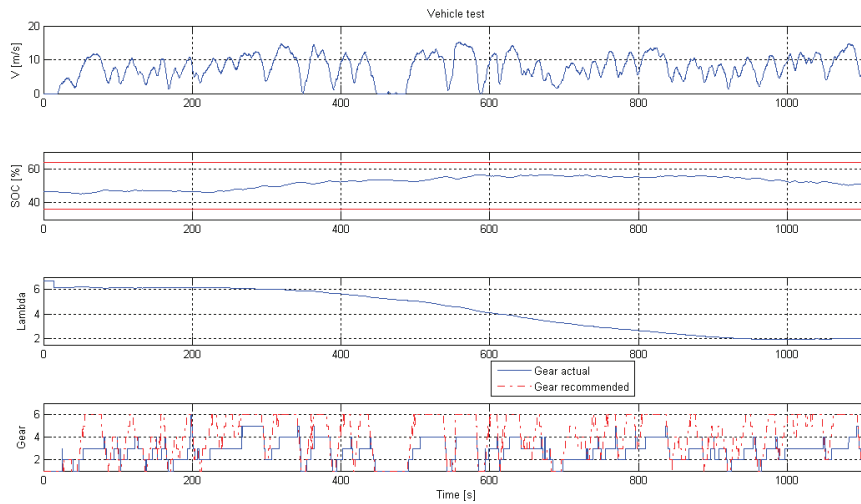


Fig 47 The SOC and control trajectories during test 1. The system is charge sustaining but the gear recommendation is often too high for comfort.

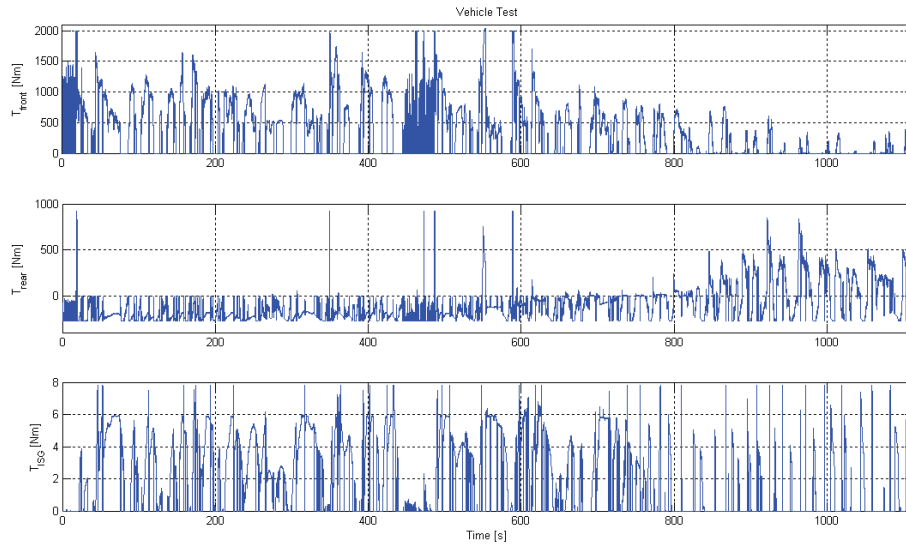


Fig 48 The torques on the converters during test 1.

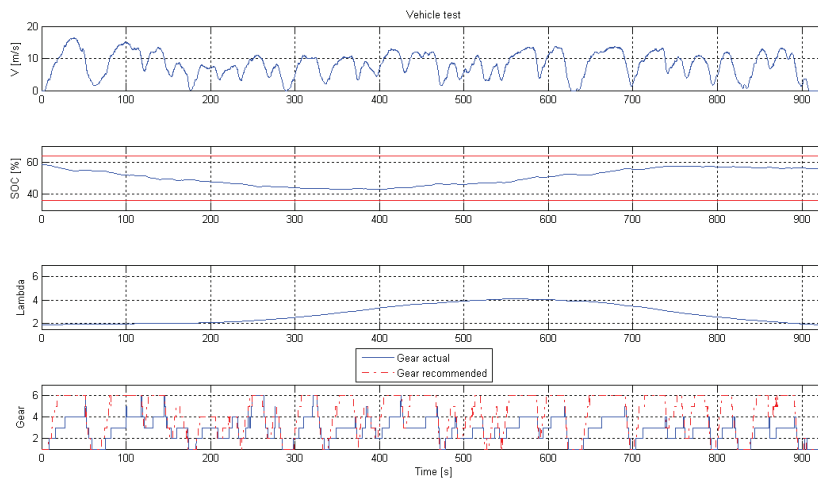


Fig 49 The SOC and control trajectories during test 2. The system is charge sustaining but the gear recommendation is often too high.

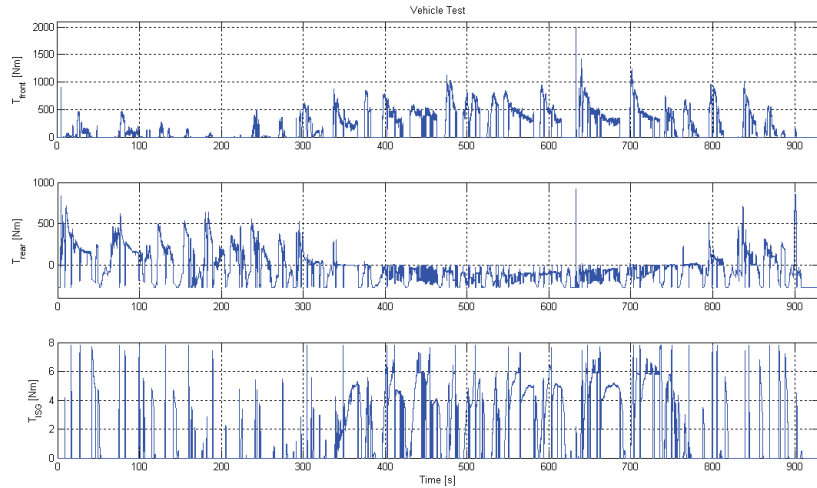


Fig 50 The torque on the converters during test 2

The results from the two tests are consistent with each other. The system keeps the SOC within the SOC window. Noticeable is how the system changes character as a result of the change in SOC and λ . When λ is large the EM produces negative torque, except during hard accelerations. As λ decreases the system shifts to using the EM more and more in the propulsion of the vehicle.

The gear recommendation consistently recommends a gear that is higher than what the driver finds comfortable. Even though the car is driveable on the gears the system recommends, using 6th gear at 30km/h may not be desirable. The algorithms strive to keep the engine speed as low as possible, down to 800rpm. No objective way to measure the driveability was used in these tests, but it was subjectively deemed good by the test-drivers.

9 Conclusion

The created system produces a satisfactory solution to the fuel minimization problem. The proposed ECMS control produces a result very close to that of DDP; 16% reduction compared to 19% on the NEDC cycle and 21% compared to 26% on the FTP-75 cycle. This is despite the fact that the ECMS doesn't control the regenerative braking and thus cannot change gear as the DDP solution does. The Stability Analysis in Section 6.2.3 also indicates that the consumption would increase for DDP if the same time discretization as in ECMS was used, thus making the difference even less. As seen in Fig 30 the ECMS uses less of the battery capacity than DDP. This is not optimal in a consumption perspective but it reduces the wear on the battery, which might be desirable in a real implementation.

The suggested adaptive controllers also perform satisfactorily. Both controllers are charge sustaining during normal driving with only a small increase in fuel consumption. The system assumes a linear relationship between the points stored in the tables. Since this is not the case, see Fig 25, some information is lost. However, the difference between the small and large tables is negligible compared to the drastically reduced memory requirements of the small tables.

The test vehicle implementation of the proposed algorithm shows that it provides charge sustenance and good driveability. The gear recommendation is often perceived as too high for comfort but it makes the driver aware of the possibility to use a higher gear and thus lower the consumption. It's however hard to make any predictions on how good the control algorithms would be in a real system since the efficiency representations of the components are constructed of assumed values and crude measurements. Since the optimization relies heavily on the efficiency of the components, there's a reason to suspect that the solution would change character if better data is used. But as implemented in the test vehicle the proposed control algorithm provide both charge sustenance and good driveability.

9.1 Future Work

The suggestion for future work is to try and devise a way to perform the optimization online. Preferably the offline calculations are made to decide the optimal gear for different equivalence factors, torques and speed. If better data isn't enough to eliminate the problem with too high gear recommendations, driveability constraints need to be added as well. It is believed that the resulting table could be transformed to a set of rules as to which gear that should be engaged. The advantage of separating the gear selection from the online optimization is that the online optimization then only would have to be carried out on the gear that is actually engaged, perhaps only in a narrow band around the last operating point. Avoiding the current interpolation has the advantage of making it possible for the algorithm to decide in which way the converters are being used, as opposed to now, when the converters are used in an almost arbitrary way between two optimums.

If no solution to the online optimization is found that uses an acceptable computational effort, the recommendation is to closer study which points should actually be included in the pre-calculated tables. In this study the point selection is done without deeper analysis, the strategy was just to try and include points in such a way that the entire torque potential of the powertrain is included.

The relatively small size of the ISG and EM in the current vehicle configuration also avoids some potential problems associated with the system performing regenerative braking. In the current

configuration the system regenerates as much as possible as soon as the brake pedal is engaged. Doing this with larger converters would lead to undesired performance. The next step would be to devise a more stable braking algorithm, if this is done within the ECMS concept or rule-based outside the optimization is also something that has to be decided.

10 References

- [1] H.Peng and Z.Filipi, "Design & Control of Hybrid Vehicles"-Course Notes, *From the Course Design & Control of Hybrid Vehicles given at College of Engineering, University of Michigan*, 12-14 Nov 2007
- [2] L.Eriksson, "Vehicle Propulsion Systems"- Lecture Notes, *From the Course Vehicle Propulsion Systems given at ISY, Linköping University*, Aug 2009
- [3] L.Guzzella and A.Sciaretta, "Vehicle Propulsion Systems – Introduction to Modeling and Optimization", Second Edition, Springer-Verlag 2007
- [4] A.Sciaretta and L.Guzzella, "Control of Hybrid Electric Vehicles", *IEEE Control Systems Magazine*, pp. 60-70, April 2007
- [5] S.Barsali, C.Miulli and A.Possenti, "A Control Strategy to Minimize Fuel Consumption of Series Hybrid Electric Vehicles", *IEEE Trans. Energy Conversion*, vol. 19, no. 1, pp. 187-195, March 2004
- [6] P.Pisu and G.Rizzoni, "A Comparative Study of Supervisory Control Strategies for Hybrid Electric Vehicles", *IEEE Trans. Control Systems Technology*, vol. 15, no. 3, pp. 506-518, May 2007
- [7] C.Musardo and G.Rizzoni, "A-ECMS: An Adaptive Algorithm for Hybrid Electric Vehicle Energy Management", *IEEE Conference on Decision and Control and the European Control Conference*, no. 44, pp. 1816-1823, Dec 2005
- [8] A.Sciaretta, M.Back and L.Guzzella, "Optimal Control of Parallel Hybrid Electric Vehicles", *IEEE Trans. Control Systems Technology*, vol. 12, no. 3, pp. 352-363, May 2004
- [9] S.Jeon, S.Jo, Y.Park and J.Lee, "Multi-Mode Driving Control of a Parallel Hybrid Electric Vehicle Using Driving Pattern Recognition", *ASME Journal of Dynamic Systems, Measurement and Control*, vol. 124, pp. 141-149, March 2002
- [10] J.Liu and H.Peng, "Modeling and Control of a Power-Split Hybrid Vehicle", *IEEE Trans. Control Systems Technology*, vol. 16, no. 6, pp. 1242-1251, Nov 2008
- [11] http://en.wikipedia.org/wiki/New_European_Driving_Cycle
- [12] <http://www.dieselnet.com/standards/cycles/ftp75.html>